LANGMUIR

Interface Components: Nanoparticles, Colloids, Emulsions, Surfactants, Proteins, Polymers

MODULATION OF INTERFACIAL HYDRATION BY CARBONYL GROUPS IN LIPID MEMBRANES

Hugo A. Pérez, Jimena del Pilar Cejas, Antonio Sebastian Rosa,
Rodrigo E Giménez, Edgardo Anibal Disalvo, and Maria Angeles Frias

Just Accepted

MODULATION OF INTERFACIAL HYDRATION BY CARBONYL GROUPS IN LIPID MEMBRANES

H.A. Pérez, J.P. Cejas, A.S. Rosa, R.E. Giménez, E.A. Disalvo, M.A. Frías

Applied Biophysics and Food Research Center (Centro de Investigaciones en Biofisica Aplicada y Alimentos, CIBAAL, National University of Santiago del Estero and CONICET) RN 9 - Km 1125, 4206 Santiago del Estero, Argentina.

Corresponding author e-mail: marafrias@hotmail.com

Summary: 8542 words; six (6) Figures.

ABSTRACT

The lack of carbonyl groups and the presence of ether bonds give the lipid interphase a different water organization around the phosphate groups that affects the compressibility and electrical properties of lipid membranes. Generalized polarization of 14:0 Diether PC in correlation with FTIR analysis indicates a higher level of polarizability of water molecules in the membrane phase around the phosphate groups both below and above T_m. This reorganization of water promotes a different response in compressibility and dipole moment of the interphase which is related to different H-bonding of water molecules with PO and CO groups.

Keyword: tetradecyl PC; DMPC; Laurdan; Generalized polarization; compressibility, FTIR, dipole potential.**Highlights:**

1

Absence of carbonyl group:

Increases the packing of water molecules around phosphate groups.

Promotes loose water in a second hydration shell in the interphase.

Eliminates coexistence of liquid condensed and liquid expanded phases.

Abbreviations: DMPC: 1,2-dimiristoyl-*sn*-glycero-3-phosphocholine; 14:0 Diether PC: 1,2-di-O-tetradecyl-*sn*-glycero-3-phosphocholine; Laurdan: 6-dodecanoyl-2-dimethyl aminonaphthalene; T_m: Transition temperature; GP: Generalized Polarization; ν_g: Center of mass; LC: Liquid Crystalline state; FWHM: full width at half-maximum.

ACKNOWLEDGEMENTS

INTRODUCTION

The hydration of lipid membranes has been a matter of discussion and analysis since its behavior determines critical properties of biological functions.[1–4] Several studies have paid attention to the contribution of water to determine thickness and area of

2

lipid membranes,[5,6] membrane structure and stability,[7] and its influence on permeability properties.[8,9]

In addition, attempts to explain the response of the lipid interphase to bio effectors has considered the thermodynamic properties of water organized around the lipids.[2,10–12] Water has been described to be organized in hydration sites such as the PO and the CO residues of the phospholipids and in between the hydrocarbon chains. Different kinds of water, in terms of energy and structure, have been identified: one strongly bound to the phosphates, one more weakly bound to the CO and another clustering around the choline groups and hydrocarbon chains.[12–17]

Recently, the hydration states of the interfacial region of lipid bilayers were investigated on the basis of the time resolved emission spectra (TRES) analysis of 6-lauroyl-2-dimethylamino naphthalene (Laurdan).[18] The number of water molecules per lipid was calculated and found to be comparable to those reported previously. In terms of bound water, the polar head groups of the lipids may include a clustered state of the water molecules.[15,19]

In this regard, previous reports have also proposed the classification of water molecules that hydrate the lipid bilayer in roughly two groups. One directly bound to the lipid molecules, known as the primary hydration shell, constituted by water molecules forming additional hydrogen bonds with other water molecules and with different hydration sites such as phosphates (PO) and carbonyl groups (CO).[15,20–22] A second hydration shell that can be easily displaced by biomolecules, enzymes, different aminoacids and chemical compounds has also been described. This water population is affected relatively easily by surface pressure and explains the insertion

3

of amino acids and proteins. Therefore, the importance of the contribution of water activity at the membrane surface on biological processes has been considered on thermodynamic backgrounds.[11,16] This implies that the energetic of the water interaction is different for each site of hydration.

For example, phosphate groups are strong hydration site and its hydration is correlated with the hydration of the acyl chains according to chain length, phase state and the presence or absence of carbonyl groups.[14]

In particular, the carbonyl groups are located in a plane running along the glycerol backbone and, in consequence, they appear to have a special influence on the interfacial properties since its affinity for water can be modified by curvature, phase state and other topological features.[17,23,24] In addition, these groups have been described to participate in the formation of defects upon deformation of the bilayer giving place to spontaneous or induced curvatures.[17] FTIR data report that in each of the sn1 and sn2 chains, the carbonyl groups (CO) present hydrated and non-hydrated distributions, as a consequence of fluctuations in CO orientation.[17,25] As reported before its presence may modulate the relative hydration of phosphate and acyl chains.[14] On this base, the comparison of ester lipids with ether lipids becomes of interest. Although ether lipids are present in bacteria, eukarya and in humans its real biological function is still not clear.[26–32] It is claimed that lipid raft formation is related to this kind of lipids.[33] Simulation of lipid bilayers composed of Ester and Ether PCs revealed that the Ester PC membrane is more compressible than that for Ether PC. This behavior was attributed to different water order and dynamics around the head group region in the Ether PC membrane.[34]

It has been reported that nanoconfined water shows a strong anisotropy[35,36] and its dielectric constant is surprisingly low (c.a. 10).[37,38] Therefore, the changes in water distribution due to the absence or presence of CO groups would affect the dielectric properties of the lipid bilayer with probable effect on its response to the penetration and stabilization of oligo peptides or aminoacids. In the region at which water may reach the ester carbonyl plane different populations of water clusters are present.[15,39] Laurdan locates in the hydrophobic/hydrophilic interfacial region near the carbonyl group of the phospholipid and therefore it has been extensively used to get information about the polarity of the environment near to it and in consequence to derive hydration states.[18,40,41] However, a difficulty to accurately estimate the number of water molecules by Laurdan fluorescence is that it cannot detect molecules farther away from the probe position. This may be ascribed to the vertical position and how deep the probe can be intercalated according to lipid composition and phase state.[18] Parasassi et al proposed that fluorescence shift with temperature of Laurdan bands is caused by the presence of water molecules in the bilayer region where Laurdan locates which seems to be congruent with NMR techniques.[42] The hypothesis of the influence of water on Laurdan fluorescence is consistent with recent studies comparing the shift in lipid - cholesterol membranes with Laurdan in octanol phase doped with different amounts of water. This is taken as a clear indication that Laurdan is directly affected by water around it.[41]

The spectral shift cannot be explained by changes in the "static" dielectric constant of the phospholipid phase, due to increased water penetration. The relaxation process in the liquid crystalline phase has been ascribed to water molecules with

5

restricted mobility with respect to bulk water.[43] Therefore, it is of interest to analyze comparatively the hydration properties of membranes composed either by ester or ether PCs merging from Laurdan fluorescence and FTIR and to correlate them with the electric and compressibility properties of the lipid interphase.

In this work, monolayers and bilayers composed by DMPC and 14:0 Diether PC were studied by steady state fluorescence spectroscopy, FTIR spectroscopy, and surface pressure isotherms. It is expected that the comparison of ester and ether linked phosphatidylcholines may provide an insight on the hydration properties at lipid interphases and its consequences on mechanical, electrical and phase properties. This may be of importance to understand the biophysical properties of these membranous systems and its relevance for their biological function.

MATERIALS AND METHODS

Chemicals

1,2-dimiristoyl-*sn*-glycero-3-phosphocholine (DMPC); 1,2-di-O-tetradecyl-*sn*-glycero-3-phosphocholine (14:0 Diether PC) and 1,2-dipalmitoyl-sn-glycero-3-phosphocholine (DPPC) were purchased from Avanti Polar Lipids Inc. (Alabaster, AL). Purity of lipids were higher than >99% as checked by FTIR, UV spectroscopies and thin-layer chromatography. Stocks of phospholipid solutions in chloroform were quantified by determining inorganic phosphorus. Laurdan (6-dodecanoyl-2-dimethyl aminonaphthalene) was obtained from Molecular Probes and used without further purification. The concentration of Laurdan stock solutions in chloroform was determined by absorption spectrophotometry at 364 nm considering an absorptivity

6

coefficient of 20.000 $M^{-1}cm^{-1}$.[41] All other chemicals were of analytical grade. Solutions of 1 mM KCl (pH 5) were prepared with ultrapure water (conductivity = 0.002–0.010 mS cm^{-1}) obtained from an OSMOION 10.2 water purification system (APEMA, Buenos Aires, Argentina).

Fluorescence spectroscopy measurements

Multilamellar liposomes (MLV´s) containing Laurdan in a 1:500 Laurdan/ lipid mol/mol ratio, were obtained by hydrating the dried lipid films with Milli-Q water or 1 mM KCl solutions above the transition temperature (T_m). The suspensions were subjected to 10 minutes vortex cycles. After this procedure, MLV´s were extruded 20 times above T_m through a polycarbonate filter (pore diameter 100 nm) to prepare large unilamellar vesicle suspensions (LUV´s). The particle size of LUV´s suspension was measured by dynamic light scattering (DLS- Horiba nano particle analyzer SZ-100). The LUV population having a diameter of 100 nm with an accuracy ± 2% at 25°C was around 99%.

Steady-state emission spectra were obtained in a SLM 4800 spectrofluorometer using a 1.0 cm quartz thermostatized cell within ± 0.5ºC. The excitation wavelength was 370 nm with a slit of 2 nm. Emission was collected in suspensions with an optical density smaller than 0.05 in the range from 220 to 700 nm. Consequently, no correction for inner filter effects was needed. Emission spectra of the samples were collected between 10 to 50ºC ± 0.1ºC.

The Excitation Generalized Polarization (GP_{ex}) function was calculated from the emission intensities using Eq. (1):

$$GP_{ex} = \frac{I_{440} - I_{480}}{I_{440} + I_{480}} \qquad \text{Eq. (1)}$$

where I_{440} and I_{480} correspond to the emission maximum in the gel and the liquid crystalline state respectively.[44–47]

Spectral Center of Mass

The spectral centre of mass was calculated by Eq. (2):

$$\nu_g = \frac{\Sigma \nu_i F_i}{\Sigma F_i} \qquad \text{Eq. (2)}$$

where F_i is the emission intensity at each wavenumber (ν_i in cm^{-1}). The summations were carried over all wavenumbers where $F_i > 0$.[48]

Wavelength number of emissions can be related with the energy content per mole (E) of the substance responsible for the emission, according to

$$E = N_A hc \nu_g \qquad \text{Eq. (3)}$$

where h is Planck's constant (6.62×10^{-34} J.s), v is frequency, c is the speed of light in the medium in which the waves propagate (2.997×10^8 m s^{-1} in vacuum), ν_g the wavenumber and N_A = Avogadro's number = 6.022×10^{23} mol^{-1}.

Spectra decomposition procedure

The emission spectra of Laurdan in the LUV's were fitted with a superposition of two LN functions using the nonlinear fiting tools of the Origin 8.5 software package as reported by Bacalum et al.[49] With this procedure the components of the emission bands of Laurdan in the different conditions were evaluated. On the base of the two

8

states assumed in the GP_{ex} calculation, it provides a comparative relation with relaxed and non-relaxed states.

Time-resolved fluorescence measurements.

The Time-resolved fluorescence measures were carried out following the protocol published by Bagatolli et al.[50]

ATR-FTIR Spectroscopy

All FTIR spectra were obtained in a Thermo Scientific 6700 spectrometer assembled with an ATR accessory with controlled humidity and temperature, and with a DTGS KBr detector, connected to a system of circulation of dry air to avoid the interference of water vapor and carbon dioxide from the environment. Lipid films prepared as described above were resuspended, above the transition temperature (T_m), in a minimum volume of KCl solution to reach a 20 mM lipid suspension. Droplets (2 μL) of each suspension were placed on the diamond crystal (45° incident angle). Spectra of fully hydrated samples were taken at 18°C and 30°C ± 0.1 °C during the dehydration process. Spectra were obtained at intervals of three minutes in order to control the water content evolution following the water band intensity, the symmetric and asymmetric $-PO_2^-$ stretching band and the asymmetric stretching vibration of the methylene groups. Water content defined as $IvH_2O/IvCH_2$ was chosen as a parameter to follow the hydration states of all studied lipids including those lacking CO groups. Wavenumber position of the lipid $v_{as}CH_2$ or $v_sPO_2^-$ stretching bands was plotted as a function of $IvH_2O/IvCH_2$. Previous works showed that the measurement

9

for water content also takes into account other vibrational modes such as water scissoring band and the lipid ester band.[51]

Data were obtained after 64 scans per sample corresponding to the average of three independent assays. Spectra were analyzed with Omnic Software (version 9.1.24) and Microcal Origin program (version 8.5). These softwares mathematically process the spectra and the peak maxima were determined by the Omnic find peak function routine resulting in an accuracy of 0.1 cm^{-1} which gives statistically reliable data.[51,52]

Surface pressure and dipole potential measurements

The surface pressure (π) and dipole potential (Ψ) compression isotherms were carried out simultaneously in a KSV NIMA LB trough (surface area = 240.00 cm^2). The system was equipped with an electrobalance and a platinum Wilhelmy plate (39.24 mm^2) as surface pressure sensor. Dipole potential was measured using a KSV SPOT with a vibrating plate electrode and a steel counter electrode immersed in the subphase.[53,54] The distance between the monolayer and the electrode was carefully adjusted to minimize the noise according instrument instructions (Input range: ±-5V; sensitivity: ± 1mV; height dependency: 10 mV/mm; response time: proportional to distance but less than 1s when positioned 1 mm above monolayer). The platinum-Wilhelmy plate was cleaned by rinsing with ultra-purified water and ethanol, and was flamed in a butane torch until glowed red-hot before each assay. The trough was filled with 120 mL of 1 mM KCl solution (pH 5) which remains constant along all the assay. Previous to each assay several sweeps when done on the water surface to avoid impurities and until the borders of the meniscus were even in the whole perimeter. Accurate volumes of 5 mM lipid solution in chloroform were

10

spread on the surface, using a Hamilton micro syringe. Monolayers were stabilized during 15 min before each measurement at 15°C and 30°C ± 0.1 °C. Compression curves were carried out at a constant speed of 2 mm/min to allow stabilization of the system at each point. Data correspond to an average of at least three independent measurements with aliquots of the same stock solutions for each lipid.

The whole equipment was enclosed in an acrylic box of controlled atmosphere to minimize water evaporation and to avoid contaminations from the environment during the study. One special point is that the close compartment avoids the CO_2 contamination that may eventually change pH by CO_2 absorption at the water -air interface.

Compressibility measures

To visualize the phase properties of 14:0 Diether PC and DMPC systems, the compressibility module was calculated using Eq. (4)

$$C^{-1} = -A\left(\frac{d\pi}{dA}\right)_T \qquad\qquad Eq. (4)$$

The compressibility modulus *vs* area/molecule is defined as a quantitative measure of the monolayer state that indicates the change in the physical state, such as the coexistence of expanded-condensed phases in the film.[55–57]

Dipole potential

The dipole potential is the change in surface potential relative to the absence of lipids and is given by Eq. 5

$$\Delta V = 37.70\ \mu_\perp/A \qquad\qquad Eq.\ (5)$$

Where ΔV is the dipole potential expressed in V, A is the area per molecule in

$Å^2$/molecule and $\mu_\perp$ in Debye (D) is the molecular dipole moment perpendicular to

the lipid-water interface.[58,59] The components of $\mu_\perp$ is subdivided into the

contributions of lipid-reoriented water molecules (μ_w), lipid polar head groups (μ_{co}),

and the chain terminal dipole (μ_{hc}).[60,61]

RESULTS

Analysis of fluorescence data

A decrease of Laurdan GP_{ex} from positive to negative values is clearly observed at

the phase transition temperature for DMPC and 14:0 Diether PC (Figure 1a). Similar

to previously reported, the transition temperature is around to 2 ºC higher in the

absence of the carbonyl groups.[50] This denotes that the presence of an ether bond

affects in a similar way the properties of the membrane phase independent of the

chain length.

The displacement of the GP_{ex} curve for 14:0 Diether PC to lower values at all

temperatures is indicative that the polarity of the environment surrounding the probe

in this kind of lipids is higher than in the ester one. GP_{ex} values are evaluated

selecting a fixed wavelength in the gel and another in the liquid crystalline state of

both lipids, and calculating the relative changes in intensity at these values along the

temperature according to Eq. (1).[44–47] However, the Spectral Centre of Mass (v_g)

calculated according to the definition in Eq. 2 in M&M, displaces with temperature.

12

This is a direct measure of the energy required at each temperature for the dipolar arrangements. The values of v_g can be expressed in terms of energy (Eq. 3- Figure 1b). Thus, it is interesting to analyse the information that this shift may provide from below to above the phase transitions.

Data in Figure 1b denotes that less energy is required for 14:0 Diether PC than for DMPC indicating that the dipole environment is less rigid or has more mobility in the 14:0 Diether PC.
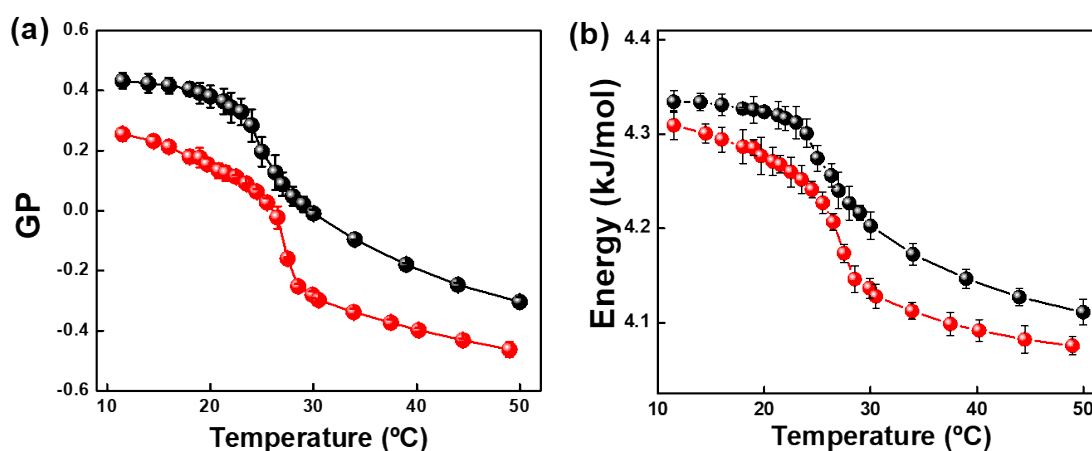

Fig. 1: Effect of temperature on GP_{ex} (a) and on Energy (b) of Laurdan in DMPC (black dots) and 14:0 Diether PC (red dots) LUV´s.

As shown in Figure 2a, the area under the curves of the Energy derivatives increase from DMPC (9.64 kJ/mol) to 14:0 Diether PC (10.06 kJ/mol) and DPPC (13.80 kJ/mol) and follows the increase of the total enthalpic change at the phase transition as measured by DSC (Fig 2b).
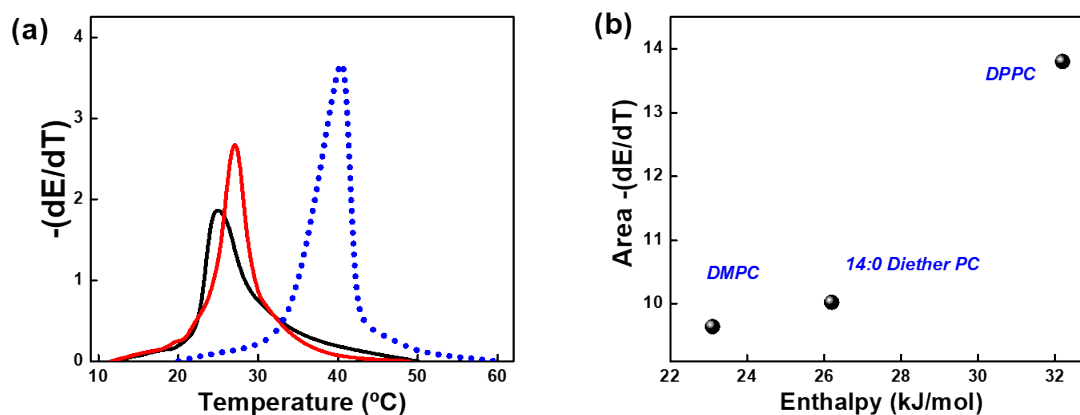
13

Fig. 2: (a) First derivative of Energy values as a function of temperature for DMPC (black line), 14:0 Diether PC (red line) and DPPC (Blue dotted line); (b) Correlation of the areas under the curves in Part (a) expressed in kJ/mol with the total enthalpic change at the phase transition measured by DSC .[62]

As described by Watanabe et al. the band obtained at 445 nm for DMPC in the gel state can be decomposed in at least two different contributions: one centered at 444 nm and another at 470 nm (Fig 3a).[18,49] When the temperature is increased and lipids go to the liquid crystalline state the band at 483 nm is significantly more intense than that appearing at 444 nm (Fig 3c).

A similar picture is obtained when, at a constant temperature below T_m, ester and ether lipids are compared. It is clearly shown in Figure 3b that the band at high wavelength corresponding to relaxable populations increases in comparison to that for DMPC. Above the T_m, the non- relaxable populations nearly disappear in 14:0 Diether PC in comparison to that in DMPC.

The deconvolution applied to emission spectrum for DMPC and 14:0 DietherPC suggests that two water populations coexists at the gel and in the liquid crystalline states of both lipids although in different ratios.

The same results and conclusions may be derived from the measures of excited state lifetimes. In the gel state the lifetime for DMPC is 6.49 ns while for 14:0 Diether PC it amounts 5.04 ns denoting a less rigid environment. In liquid crystalline state, both values decrease (4.29 ns for DMPC and 3.68 ns for 14:0 Diether PC). As observed in this state, the value for the ether lipid is lower than that for the ester one.
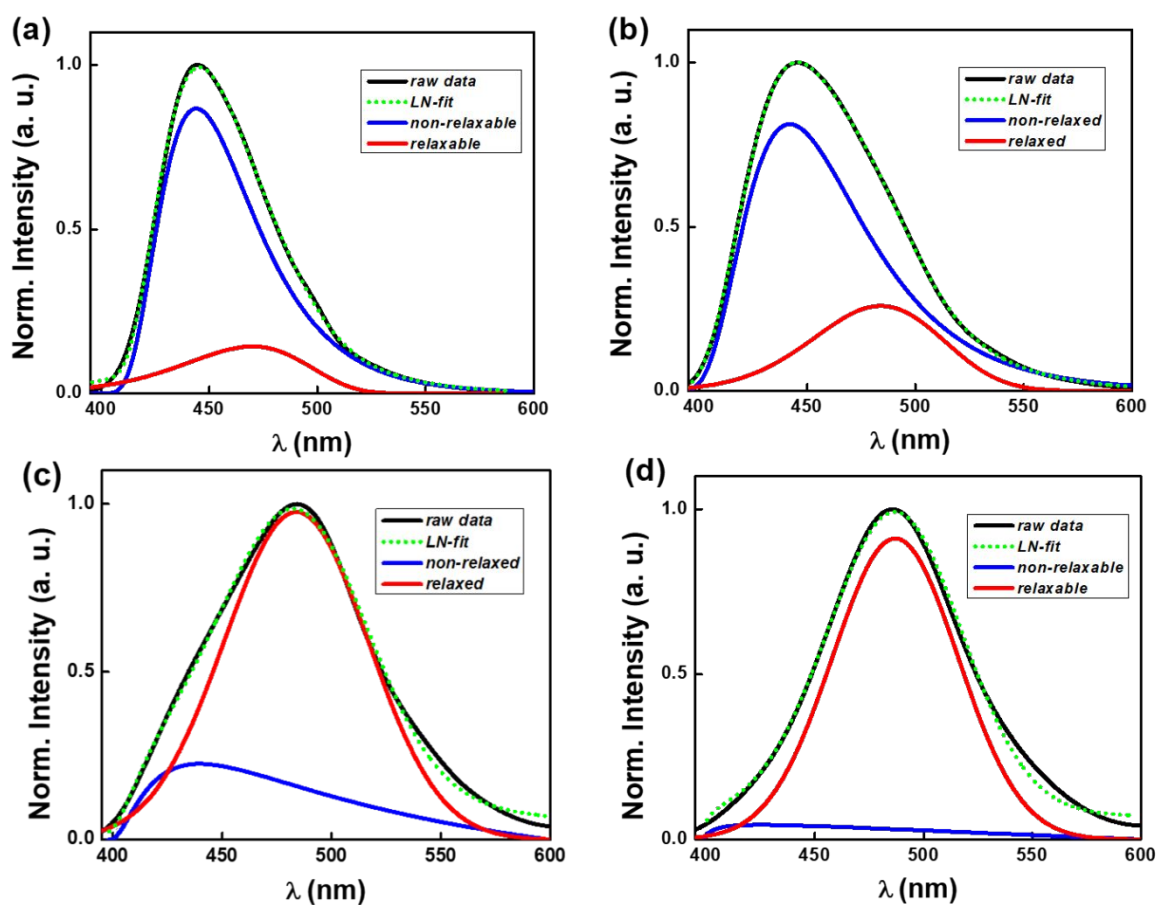
Fig. 3: Deconvolution of emission spectra for DMPC and 14:0 Diether PC. Upper panels correspond to a) DMPC and b) 14:0 Diether PC at 15 °C; lower panels correspond to c) DMPC and d) 14:0 Diether PC at 45ºC.

Laurdan relaxation takes place according to the water molecules that surround it, i.e. the components of the bands at 440 and 470 nm can be taken as an indirect measure of water with different properties to relax (non-relaxable and relaxable populations). The comparison of GP_{ex} values and energy values (Fig 1a and 1b) on one hand and the deconvolution of fluorescence bands on the other, indicates the coexistence of environments of different polarity which may be related to differences in the distribution of water dipoles of different energy of interaction by H bonds between them and with the lipid groups such as PO and CO, in accordance to Alarcon et al.[15] In order to get a molecular insight of the mesoscopic description obtained by fluorescence and ascribed to water environments in ether and ester PC bilayers, FTIR analysis were done analyzing the frequencies of the phosphate groups below and above the phase transition temperature for both lipids. This is presented in the next section.

FTIR analysis

The FTIR analysis is based on the fact that the frequency of vibration (ν) of a given bond is expressed by the equation

$$\nu = \frac{1}{2}\pi\sqrt{\frac{k}{\mu}} \qquad\qquad \textbf{Eq (6)}$$

16

Where k is the force constant of the bond and μ the reduced mass of the two atoms

forming the bond. The frequency decrease is then a direct measure of the bond

weakening. When a group concerts a hydrogen bond with an adjacent molecule, the

frequency of the bond decreases. The decrease in the frequency of the phosphate

stretching vibrations with water content is an indication of the amount and the energy

of the hydrogen bonds that the phosphate groups may form.[14,51] Thus, FTIR analysis

provides a microscopic picture of that derived from mesoscopic description done

with Laurdan fluorescence described in the previous section.

Figure 4 shows that the phosphate frequencies are lower for 14:0 Diether PC than

for DMPC both below (18°C) and above (35°C) the phase transition temperature. In

Fig. 4a it is observed a decrease for the 14:0 Diether PC PO_2^- symmetric frequencies

in comparison with DMPC. In Figure 4b the frequency vibration of asymmetric PO_2^-

is also analyzed giving the same results as observed for the symmetric one.[14] The

lower frequencies in 14:0 Diether PC in comparison to DMPC can be ascribed to a

stronger H bond interaction of PO_2^- groups with water molecules at the interphase.
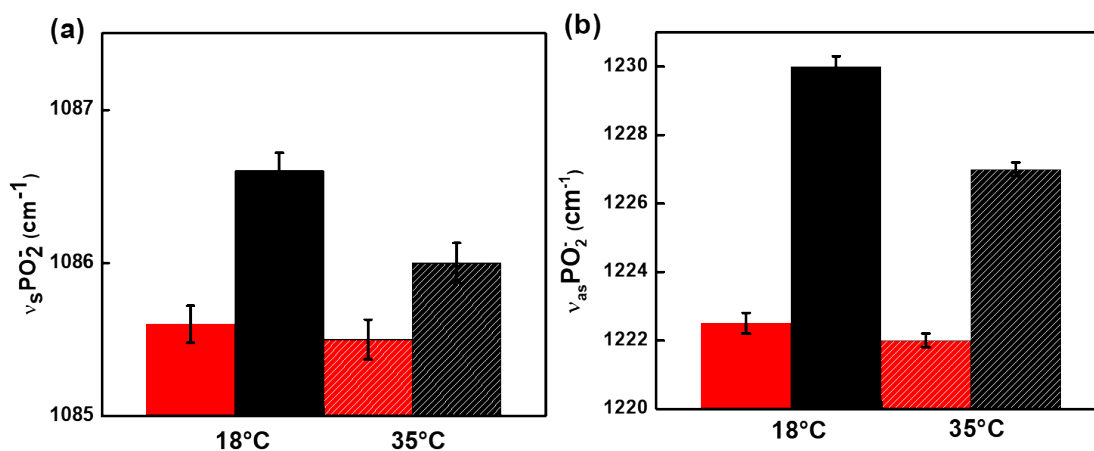
Fig. 4: Comparison of symmetric a) and asymmetric b) phosphate vibration frequencies for fully hydrated 14:0 Diether PC (red) and DMPC (black) at 18 ºC and 35 ºC. The error bars represent the standard deviation of three measurements.

The results of FTIR indicating that water molecules are strongly bound to the phosphate group in the absence of CO are congruent with the increase in more polarizable water observed with Laurdan.

Monolayer properties

The change in hydration state described in the previous section may have consequences on the physical properties of lipid interphase. Thus, the influence of the carbonyl group on the compressibility and the dipole moment of lipid monolayers was analyzed.

Compressibility properties.

The compressibility modulus (C^{-1}) *vs* area of DMPC and 14:0 Diether PC are compared at 15ºC and 30ºC (Fig. 5a). C^{-1} was calculated from the data in Figure S1 using equation 3. In both cases, a jump in C^{-1} is observed between 110 and 120 $Å^2$ for 14:0 Diether PC at 15°C and 30°C, being both values higher than those observed for DMPC at similar temperatures.

The compressibility *vs*. surface pressure curve in Fig. 5b shows that, at low pressures, the behavior of the ester and ether lipids are similar. However, a noticeable difference is observed at 20 mN/m in which DMPC shows a broad peak between 20 and 29 mN/m while ether lipid shows a continuous increase up to 31

18

mN/m. Data of lipids above the transition temperature are shown in supplementary
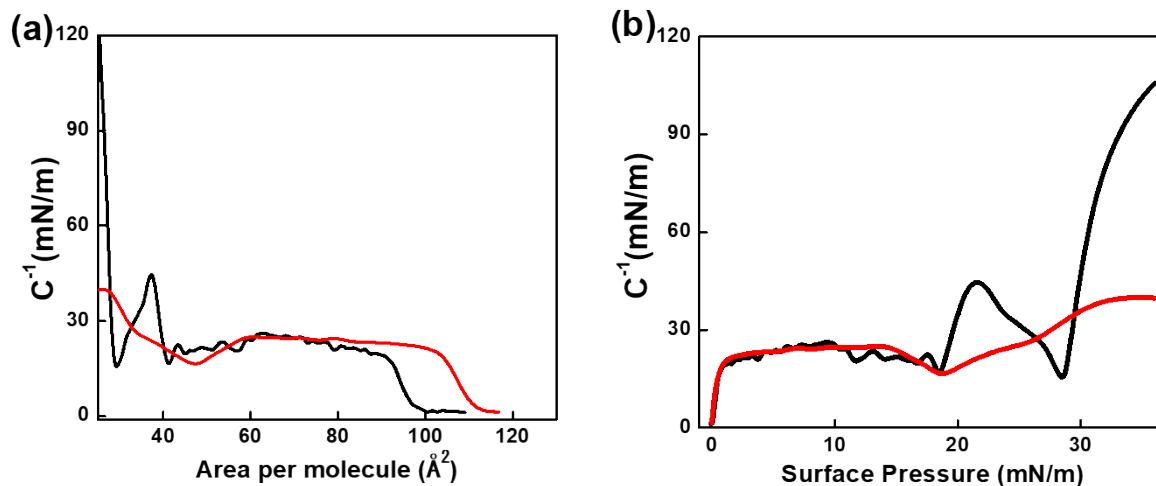
material (S2).

Fig. 5: Compressibility modulus *vs.* area per molecule (a) and Compressibility

modulus *vs* Surface Pressure (b) for DMPC (black lines) and 14:0 Diether PC (red

lines) at 15 °C.

Dipole potential and Molecular dipole moment ($\mu_\perp$):

In Figure 6a, it is observed that dipole potential per unit area of DMPC and of 14:0

Diether PC increases with surface pressure. In Figure 6b, the values of molecular

dipole moment ($\mu_\perp$) defined in M & M, are plotted as a function of the surface

pressure. It is observed that the curve corresponding to 14:0 Diether PC (red line)

falls below that of DMPC (black line) congruent with the lack of a population of

dipoles (CO groups). When plotted in a normalized way (inset Fig. 6b) it is observed

that both curves overlap until a pressure of 20 mN/m, at which the dipole moment

19

reaches a constant limit value of around 0.3 - 0.4 D (Fig. 6b), coincident with the peak of compressibility observed for DMPC in Fig. 5b.

In contrast, dipole moment still decreases at higher pressures in 14:0 Diether PC suggesting the loss of dipoles or a further rearrangement of dipoles at the interphase.
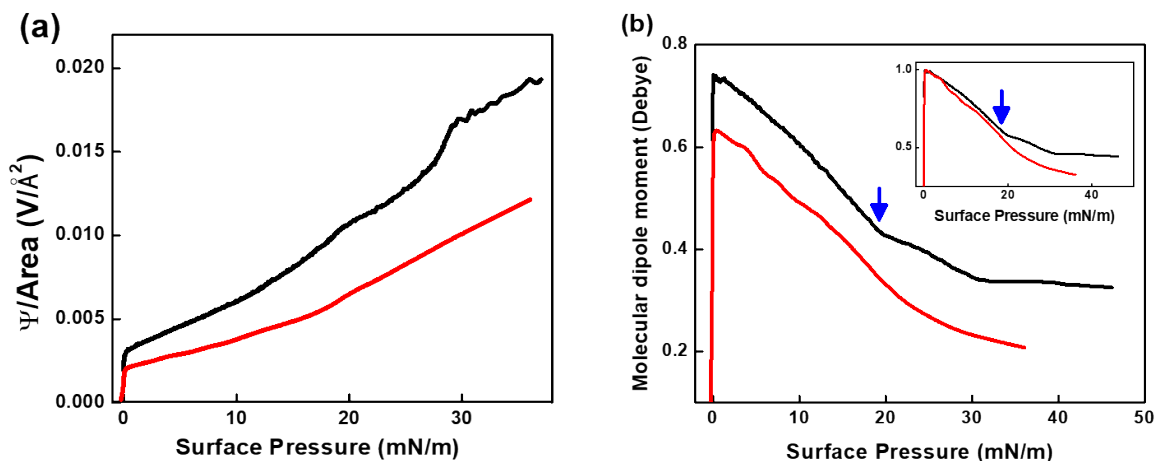

Fig. 6: Dipole potential per unit area (a) and Molecular dipole moment (b) *vs* Surface Pressure (mN/m) for DMPC (black line), 14:0 Diether PC (red line). Inset: molecular dipole moment normal to the membrane plane *vs* Surface pressure for DMPC (black line), 14:0 Diether PC (red line) at 15°C.

DISCUSSION

The displacement of the transition to higher temperatures accounts for a higher requirement of energy of ether PC than for DMPC. This energy increase could be due to stronger interactions between the lipids when the carbonyl group is absent. A possible explanation is that the lack of carbonyl group has a similar effect than an increase in the chain length. This is sustained by the observation that the transition

20

temperatures follow the trend 14:0 PC - 14:0 di ether PC - 15:0 PC - 16:0 PC - 16:0

Di ether PC.[50,62]

The enthalpy transition follows the same trend denoting an increase from 23 kJ/mol

to 26 kJ/mol to 33 kJ/mol (Figure 2b). Estimates of C_p (heat capacity) revealed that

a significant amount of water may be present in the hydrocarbon region.[12,63]

Thus, the total enthalpy change (ΔH_t) measured by calorimetry would be given by

the energy corresponding to the fusion of lipid lattice reticule (ΔH_l) and that related

to the hydration of the lipids (ΔH_h)

$$\Delta H_t = \Delta H_l + \Delta H_h \qquad (7)$$

According to Epand et al., each CH_2 in each acyl chain contributes to the enthalpic

change (ΔH_{CH2}) with 2-3 kJ/mol.[64] If it is considered that the first $6CH_2$ do not

contribute to the enthalpy change,[65] the total enthalpy (ΔH_t) for DMPC can be

calculated by

$$\Delta H_t = 2(n - n_c)\Delta H_{CH_2} + \Delta H_W \qquad (8)$$

where ΔH_t = 23 kJ/mol, n= 14 for DMPC, n_c= 6 and ΔH_{CH2}= 2 kJ/mol.   The

contribution of water (ΔH_w) as calculated from equation (8), is approx. 9 kJ/mol.

Similarly, considering that in the case of 14:0 Diether PC the chain is one CH_2 longer

due to the absence of the ester union, ΔH_w is equal to 10 kJ/mol. In both case the

values are comparable to the area value obtained under the curve of Figure 2. As

the Energy values (Figure 1b) account for changes in the water environment, the

changes in the area under curves of Figure 2a would correspond to the contributions of the water molecules to the transition of the different lipids.

1.-Relaxable and non relaxable populations as measured by FTIR and Laurdan fluorescence.

The bands obtained by deconvolution in Figure 3 can be ascribed to Laurdan molecules which experiment different degree of dipole relaxation in relation to the surrounding water. Thus, it can be taken as an indirect indication of water molecules organized in populations having low and high restricted mobility identified as relaxable and non relaxable respectively.

The population of water dipoles with more propensity to relax increases in 14:0 Diether PC in comparison to DMPC at the same temperature, suggesting that the *water shell* is less tightly bound for 14:0 Diether PC than in DMPC or at least it has more mobility as inferred from the decrease in relaxation times. A higher level of polarizable water molecules around the probe (*relaxable population*) cannot be necessarily interpreted as free water, but as water that has less restriction to rotate. Hence, the contribution to the Cp will be higher, congruent with the enthalpic change shown above. The fluorescent results with Laurdan are compatible with those reported with other probes in the sense that solvent reorientation in ester PC membranes is slow compared to the ether lipid, due to the water bound to the carbonyl groups by H bonds.[66]

This behavior can be further sustained considering the changes in PO_2^- symmetric and asymmetric frequencies. It is well known that DMPC has two hydration sites in

22

the headgroup region (PO_2^- and CO) and 14:0 Diether PC only one (PO_2^-).[16] Results in Figure 4, showing an increase the PO stretching frequency, indicate that the strength of the water-phosphate H-bond is higher in 14:0 Diether PC. Thus, in the absence of carbonyl group, a stronger association of water with the phosphate groups is present. This experimental evidence can be explained considering that in DMPC, water molecules could bind simultaneously to PO_2^- and CO by H bonds, in the same lipid molecule forming a water bridge as proposed by Ohto et al.[67]

Complementary simulation studies using different force fields and water models have also indicated that the chemical nature of lipid chains affects the dynamics of the bilayer lipid water interface. They provide evidences that different relaxation rate populations in the water molecules are relevant in understanding the structural or orientational heterogeneity of interface water near DMPC above the phase transition temperature. Although no analysis in the gel state or in ether lipid are available, those data together with the present ones are key elements to understand the thermodynamic of lipid interphases in terms of dynamic properties since them appear correlated with the phase states of the bilayers. A slow relaxation of interfacial water is attributed to the presence of a strong interaction at a location close to carbonyl groups as seen in time-resolved fluorescence study.

Chemically confined water molecules near lipid membranes are governed by dynamical heterogeneities originated from different kinds of hydrogen bonds Different kinds of confined water may coexist near membranes at room temperature relevant to the phase transitions of lipid bilayers as deduced from the GP data. Different water populations may reside within a layer of 0.3 to 0.8 nm along the

23

bilayer normal. The oxygen-oxygen and oxygen–hydrogen angles deviate from tetrahedral array found in bulk water which may produce an free energy excess (surface tension) In 14:0 Diether PC, these water molecules would be linked only to the PO_2^- group making the H -bond stronger but having the possibility to rotate around the H-bond, as graphically represented in the next scheme 1:
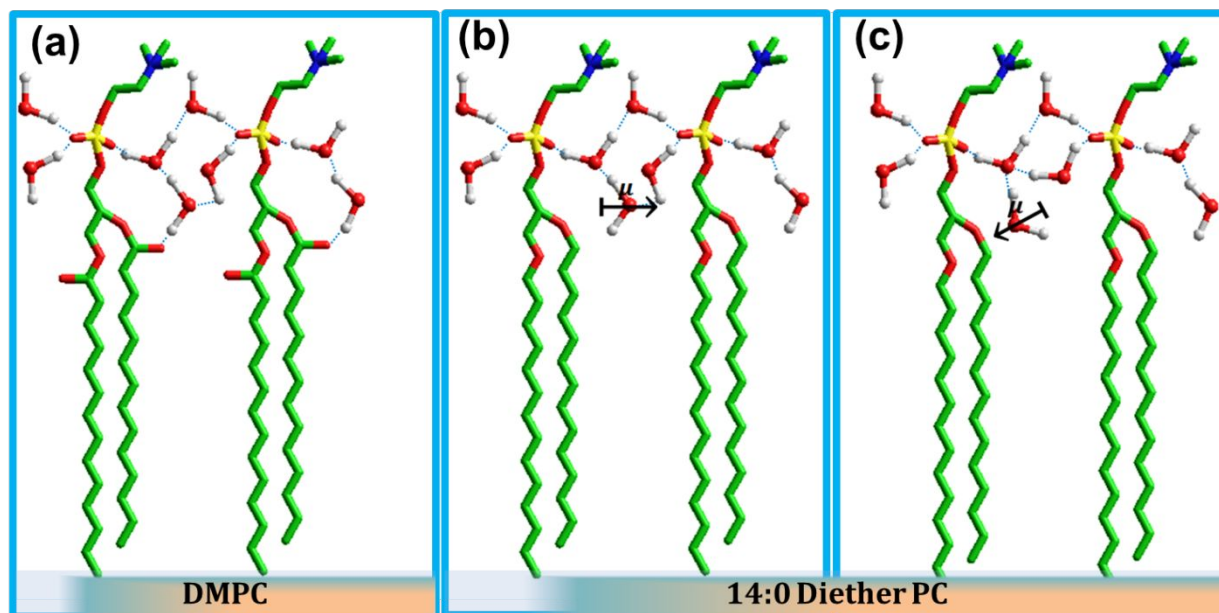
Scheme 1: The left hand (a) scheme represents the DMPC molecule showing the formation of an intramolecular water bridge between a PO and a CO group. In the central scheme (b), the water bridge is broken due to the absence of CO group. The water bound to the PO can rotate around the H-bond given as a result a reorientation of the water dipole of 90º with respect to the membrane plane (right-handed scheme-c).

24

The increase in rotational degrees of freedom of water molecules hydrating the PO group in 14:0 Diether PC would explain the increase in polarizability observed by fluorescence and the ΔH values.

The combination of FTIR and fluorescence values indicates that there are two water arrangements in the lipid interphase which is changed whether carbonyl is present or not.

According to Eq. 1, GP_{ex} can be written as:

$$GP_{ex} = \left({I_{440}}\middle/{I_T}\right) - \left({I_{480}}\middle/{I_T}\right) = X_{gel} - X_{lc}$$

with $I_T = I_{440} + I_{490}$.

Then, the terms X_{gel} and X_{lc} denote the fractions that relax at 440nm and 480nm respectively. The inspection of Figure 1a indicates that these two fractions do not take a value equal to one, which would denote that 100% of the population relax at 440 nm (x_{gel} =1; x_{lc} =0) or at 480 nm (x_{gel} =0; x_{lc} = 1). The values different from 1 above and below T_m denotes that a mixture of the two populations coexists in both phase states.

The comparison of the values of X_{gel} and X_{lc} between DMPC and 14:0 Diether PC indicates that below T_m 40% of the population relax at high energy in DMPC and only 20% in the 14:0 Diether PC. Above T_m the values are 40% and 50% respectively.

A more consistent information is obtained from v_g that is calculated considering the whole band of emission at different temperatures and that can be expressed in terms

25

of energy and therefore it may be correlated with calorimetric values. According to the description in the scheme, water molecules acquire additional rotational degrees of freedom in the absence of CO that contribute to the transition.

2.-Compressibility and dipole moment properties.

Based on the scheme given above, it is possible to rationalize the compressibility and dipole moment data described in Fig. 5 and 6. The small increase of the transition temperature observed for 14:0 Diether PC in comparison to DMPC, can be explained considering that in this last case, the presence of carbonyl groups would be a steric hindrance for lipid packing. Also, the scheme denotes the possibility of forming intermolecular water bridges between CO and PO groups.

In the absence of CO, hydrocarbon chains are slightly longer and hence there would be an increase of the dispersion forces between them explaining the increasing in T_m. This is manifested in the calculation of ΔH_l in which considering ether PC with an additional CH_2, and $n_c = 6$ a consistent value of ΔH_w, in equation 7 is obtained. Data in Figure 5a demonstrate that DMPC is more compressible than ether lipid. This behavior has been also observed by MD simulations comparing DPPC with 16:0 Diether PC (DHPC).[18] In Fig. 5b DMPC profile of C^{-1} curves vs. surface pressure is strongly altered in the absence of the CO groups. It presents a peak centered at 20 mN/m that according to Yu et al involves two different contributions in the lipid headgroup region.[70] The maximum for DMPC corresponds to the coexistence of the LE and LC phase of the surface pressure vs area per lipid isotherm (Figure S1). In contrast, in the same range of surface pressure, 14:0 Diether PC shows a continue

26

increase in C^{-1} that might be due to a rearrangement of the water molecules with pressure with the possibility to rotate.

So, how is this lower compressibility in the ether lipid compatible with a tighter hydration in the phosphate group and more less-bounded water around it? As reported before, water can penetrate up to the carbonyl region.[39,71] In its absence, chains are more packed as inferred from the slight increase in T_m in the direction of a chain length increase (Figure 2b). An interpretation is that, in the absence of CO, water "sees" a more hydrophobic wall that imposes an increased order that would favor the hydrophobic interaction between adjacent chains, expelling water which, according to FTIR data, is relocalized around the phosphate groups. The new water atmosphere around these groups seems to be more polarizable according to the decrease in GP_{ex} and ascribed to water that has gained rotational degree of freedom (see scheme above). The rotation of these water dipoles could account for the increase in polarization. The parameters that, in principle, would reflect these orientational changes are dipole potential per unit area and dipole moment, analyzed in Figure 6a and b. According to the scheme above, the orientation of the water molecule bound to the phosphate can rotate changing drastically the orientation of the dipole. In DMPC in which the water is fixed to PO and CO sites, the surface pressure would reduce the number of dipoles per unit area until a critical area is reached. At this point, DMPC cannot be further compressed and therefore reaches a constant dipole moment value coincident when the lipids enter in the liquid condensed state. However, in 14:0 Diether PC compression above 20mN/m can still produce a reorientation of the dipole giving a continuous decrease in dipole moment.

27

This population of water dipoles would be that showing an increased mobility and polarizability as inferred from Laurdan fluorescence measures given above. This difference has been shown to be a contribution of water dipole orientation,[54] and hence an increase in water order due to compression.

As reported by MD analysis, water in the DPPC headgroup is less ordered than 16:0Diether PC until approximately 13 Å from the centre of the bilayer. Water near the ether PC headgroups appears to be less mobile than water near the headgroups of DPPC.[34] This is apparently in contrast with the present results and analysis. However, as shown by FTIR, in the absence of CO groups water in the headgroup region seems to better associated with phosphate, which would be in agreement with the MD results. However, although this increase would reduce lateral diffusion it would increase rotational water orientation.[34]

In terms of comparing phase states in monolayers and bilayers, it should be considered that the surface pressure in bilayers has been calculated to be around 30-35 mN/m.[72]At this surface pressure, according to Figure S1, both lipids are entering at the solid phase (see arrow). However, the area per lipid is higher for the ether PC in comparison to the ester lipid. Thus, in ether PC combines the highly order state in the acyl chain region (compatible with the gel phase) with a high degree of hydration in the phosphate region (compatible with the liquid crystalline state). This combination has also been described in interdigitated phases.[73,74]

1
2
3
4
5
6
7
8
9
10
11
12
13
14
15
16
17
18
19
20
21
22
23
24
25
26
27
28
29
30
31
32
33
34
35
36
37
38
39
40
41
42
43
44
45
46
47
48
49
50
51
52
53
54
55
56
57
58
59
60

CONCLUSIONS

The lack of carbonyl groups gives the ether lipids different surface physical chemical properties when compared with the diacyl/ester PC. The main differences are:

.- a change in the hydration state visualized as a stronger interaction of water with the phosphates together with an increase of more polarizable water.

.- an increase in the cohesion between lipids indicating more propensity to form condensed phase at lower pressures;

.- Water with different relaxation properties around the head groups can be modulated by the presence of carbonyl groups with consequences on dipole surface potential and compressibility properties.

.- Confined water molecules in membrane interphase could play a key role in the structure, function and dynamics of many biological systems. The different coexistence of relaxable and non relaxable water molecules may have important consequences on the polarizability and dielectric properties of the lipid interphase which greatly affect the binding of ions and charge solutes. With this in mind, it can be speculated that the variation of the different exposure of CO groups at the interphase would affect the surface charge potential (zeta potential) affecting electrostatic forces driving the lipids protein interaction. Further experiments should be design in order to test this hypothesis

29

REFERENCES

(1)   Sparr, E.; Wennerström, H. Responding Phospholipid Membranes - Interplay between Hydration and Permeability. *Biophys. J.* **2001**, *81* (2), 1014–1028.

(2)   Damodaran, S. Water Activity at Interfaces and Its Role in Regulation of Interfacial Enzymes: A Hypothesis. *Colloids Surfaces B Biointerfaces* **1998**, *11* (5), 231–237.

(3)   Damodaran, K. V.; Merz, K. M. A Comparison of DMPC- and DLPE-Based Lipid Bilayers. *Biophys. J.* **1994**, *66* (4), 1076–1087.

(4)   Luckey, M. *Membrane Structural Biology: With Biochemical and Biophysical Foundations*; Cambridge University Press, 2014.

(5)   Parsegian, V. A.; Rand, R. P.; Rau, D. C. Osmotic Stress, Crowding, Preferential Hydration, and Binding: A Comparison of Perspectives. *Proc. Natl. Acad. Sci. U. S. A.* **2000**, *97* (8), 3987–3992.

(6)   Tristram-Nagle, S.; Nagle, J. F. Lipid Bilayers: Thermodynamics, Structure, Fluctuations, and Interactions. *Chem. Phys. Lipids* **2004**, *127* (1), 3–14.

(7)   Roy, A.; Dutta, R.; Kundu, N.; Banik, D.; Sarkar, N. A Comparative Study of the Influence of Sugars Sucrose, Trehalose, and Maltose on the Hydration and Diffusion of DMPC Lipid Bilayer at Complete Hydration: Investigation of Structural and Spectroscopic Aspect of Lipid-Sugar Interaction. *Langmuir* **2016**, *32* (20), 5124–5134.

(8)   Disalvo, E. A.; De Gier, J. Contribution of Aqueous Interphases to the Permeability Barrier of Lipid Bilayers for Non-Electrolytes. *Chem. Phys. Lipids* **1983**, *32* (1), 39–47.

(9)   Del Regno, A.; Notman, R. Permeation Pathways through Lateral Domains in Model Membranes of Skin Lipids. *Phys. Chem. Chem. Phys.* **2018**, *20* (4), 2162–2174.

(10)   Wennerström, H.; Sparr, E. Thermodynamics of Membrane Lipid Hydration. *Pure Appl. Chem.* **2003**, *75* (7), 905–912.

(11)   Disalvo, E. A.; Martini, M. F.; Bouchet, A. M.; Hollmann, A.; Frías, M. A. Structural and Thermodynamic Properties of Water-Membrane Interphases: Significance for Peptide/Membrane Interactions. *Adv. Colloid Interface Sci.* **2014**, *211*, 17–33.

(12)   Pinto, O. A.; Disalvo, E. A. A New Model for Lipid Monolayer and Bilayers Based on Thermodynamics of Irreversible Processes. *PLoS One* **2019**, *14* (4), e0212269.

(13)   Pinto, O. A.; Bouchet, A. M.; Frías, M. A.; Disalvo, E. A. Microthermodynamic

Interpretation of Fluid States from FTIR Measurements in Lipid Membranes: A Monte Carlo Study. *J. Phys. Chem. B* **2014**, *118* (35), 10436–10443.

(14) Rosa, A. S.; Edgardo; Disalvo, E.; Cejas, J. P.; Frías, M. A. Correlation between the Hydration of Acyl Chains and Phosphate Groups in Lipid Bilayers: Effect of Phase State, Head Group, Chain Length, Double Bonds and Carbonyl Groups. *Biochim. Biophys. Acta - Biomembr.* **2019**.

(15) Alarcón, L. M.; de los Angeles Frías, M.; Morini, M. A.; Belén Sierra, M.; Appignanesi, G. A.; Anibal Disalvo, E. Water Populations in Restricted Environments of Lipid Membrane Interphases. *Eur. Phys. J. E* **2016**, *39* (10).

(16) Disalvo, E. A.; Lairion, F.; Martini, F.; Tymczyszyn, E.; Frías, M.; Almaleck, H.; Gordillo, G. J. Structural and Functional Properties of Hydration and Confined Water in Membrane Interfaces. *Biochim. Biophys. Acta - Biomembr.* **2008**, *1778* (12), 2655–2670.

(17) De Los Angeles Frías, M.; Disalvo, E. A. Configuration of Carbonyl Groups at the Lipid Interphases of Different Topological Arrangements of Lipid Dispersions. *Langmuir* **2009**, *25* (14), 8187–8191.

(18) Watanabe, N.; Suga, K.; Slotte, J. P.; Nyholm, T. K. M.; Umakoshi, H. Lipid-Surrounding Water Molecules Probed by Time-Resolved Emission Spectra of Laurdan. *Langmuir* **2019**, *35*, 6762–6770.

(19) Disalvo, E. A.; Pinto, O. A.; Martini, M. F.; Bouchet, A. M.; Hollmann, A.; Frías, M. A. Functional Role of Water in Membranes Updated: A Tribute to Träuble. *Biochim. Biophys. Acta - Biomembr.* **2015**, *1848* (7), 1552–1562.

(20) Pasenkiewicz-Gierula, M.; Takaoka, Y.; Miyagawa, H.; Kitamura, K.; Kusumi, A. Hydrogen Bonding of Water to Phosphatidylcholine in the Membrane as Studied by a Molecular Dynamics Simulation: Location, Geometry, and Lipid-Lipid Bridging via Hydrogen-Bonded Water. *J. Phys. Chem. A* **1997**, *101* (20), 3677–3691.

(21) Calero, C.; Franzese, G. Membranes with Different Hydration Levels: The Interface between Bound and Unbound Hydration Water. *J. Mol. Liq.* **2019**, *273*, 488–496.

(22) Lee, E.; Kundu, A.; Jeon, J.; Cho, M. Water Hydrogen-Bonding Structure and Dynamics near Lipid Multibilayer Surface: Molecular Dynamics Simulation Study with Direct Experimental Comparison. *J. Chem. Phys.* **2019**, *151* (11), 114705.

(23) McIntosh, T. J.; Simon, S. A.; Dilger, J. P. Location of the Water-Hydrocarbon Interface in Lipid Bilayers. *From Model Membr. to Isol. cells. G. Benghe, Ed. CRC Press. Boca Raton, FL* **1989**, 1–13.

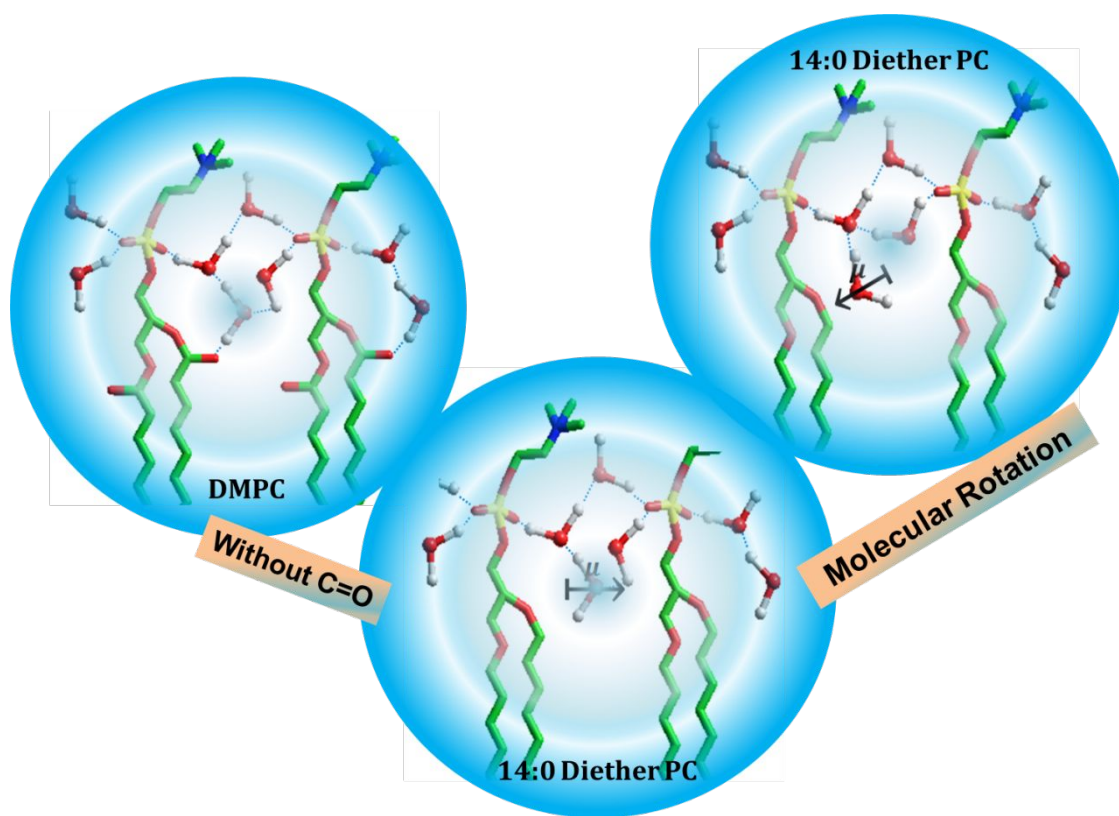(24) Cejas, J. P.; Rosa, A. S.; Pérez, H. A.; Alarcón, L.; Menéndez, C.;

Appignanesi, G. A.; Disalvo, A.; Frías, M. A. Effect of Xanthone and 1-Hydroxy Xanthone on the Dipole Potential of Lipid Membranes. *Colloids Interface Sci. Commun.* **2018**, *26* (June), 24–31.

(25) Blume, A.; Hiibner, W.; Messner, G. Fourier Transform Infrared Spectroscopy Of13c=0-Labeled Phospholipids Hydrogen Bonding To Carbonyl Groups. *Biochemistry* **1988**, *27* (21), 8239–8249.

(26) Sindelar, P. J.; Guan, Z.; Dallner, G.; Ernster, L. The Protective Role of Plasmalogens in Iron-Induced Lipid Peroxidation. *Free Radic. Biol. Med.* **1999**, *26* (3–4), 318–324.

(27) Braverman, N. E.; Moser, A. B. Functions of Plasmalogen Lipids in Health and Disease. *Biochim. Biophys. Acta - Mol. Basis Dis.* **2012**, *1822* (9), 1442–1452.

(28) Kuerschner, L.; Richter, D.; Hannibal-Bach, H. K.; Gaebler, A.; Shevchenko, A.; Ejsing, C. S.; Thiele, C. Exogenous Ether Lipids Predominantly Target Mitochondria. *PLoS One* **2012**, *7* (2), 1–12.

(29) de Rosa, M.; de Rosa, S.; Gambacorta, A.; Minale, L.; Bu'lock, J. D. Chemical Structure of the Ether Lipids of Thermophilic Acidophilic Bacteria of the Caldariella Group. *Phytochemistry* **1977**, *16* (12), 1961–1965.

(30) Guler, S. D.; Ghosh, D. D.; Pan, J.; Mathai, J. C.; Zeidel, M. L.; Nagle, J. F.; Tristram-Nagle, S. Effects of Ether vs. Ester Linkage on Lipid Bilayer Structure and Water Permeability. *Chem. Phys. Lipids* **2009**, *160* (1), 33–44.

(31) Haas, N. S.; Sripada, P. K.; Shipley, G. G. Effect of Chain-Linkage on the Structure of Phosphatidyl Choline Bilayers. Hydration Studies of 1-Hexadecyl 2-Palmitoyl-Sn-Glycero-3-Phosphocholine. *Biophys. J.* **1990**, *57* (1), 117–124.

(32) Koivuniemi, A. The Biophysical Properties of Plasmalogens Originating from Their Unique Molecular Architecture. *FEBS Lett.* **2017**, *591* (18), 2700–2713.

(33) Pike, L. J.; Han, X.; Chung, K. N.; Gross, R. W. Lipid Rafts Are Enriched in Arachidonic Acid and Plasmenylethanolamine and Their Composition Is Independent of Caveolin-1 Expression: A Quantitative Electrospray Ionization/Mass Spectrometric Analysis. *Biochemistry* **2002**, *41* (6), 2075–2088.

(34) Kruczek, J.; Saunders, M.; Khosla, M.; Tu, Y.; Pandit, S. A. Molecular Dynamics Simulations of Ether- and Ester-Linked Phospholipids. *Biochim. Biophys. Acta - Biomembr.* **2017**, *1859* (12), 2297–2307.

(35) Zhang, C.; Gygi, F.; Galli, G. Strongly Anisotropic Dielectric Relaxation of Water at the Nanoscale. *J. Phys. Chem. Lett.* **2013**, *4* (15), 2477–2481.

(36) De Luca, S.; Kannam, S. K.; Todd, B. D.; Frascoli, F.; Hansen, J. S.; Daivis, P. J. Effects of Confinement on the Dielectric Response of Water Extends up

32
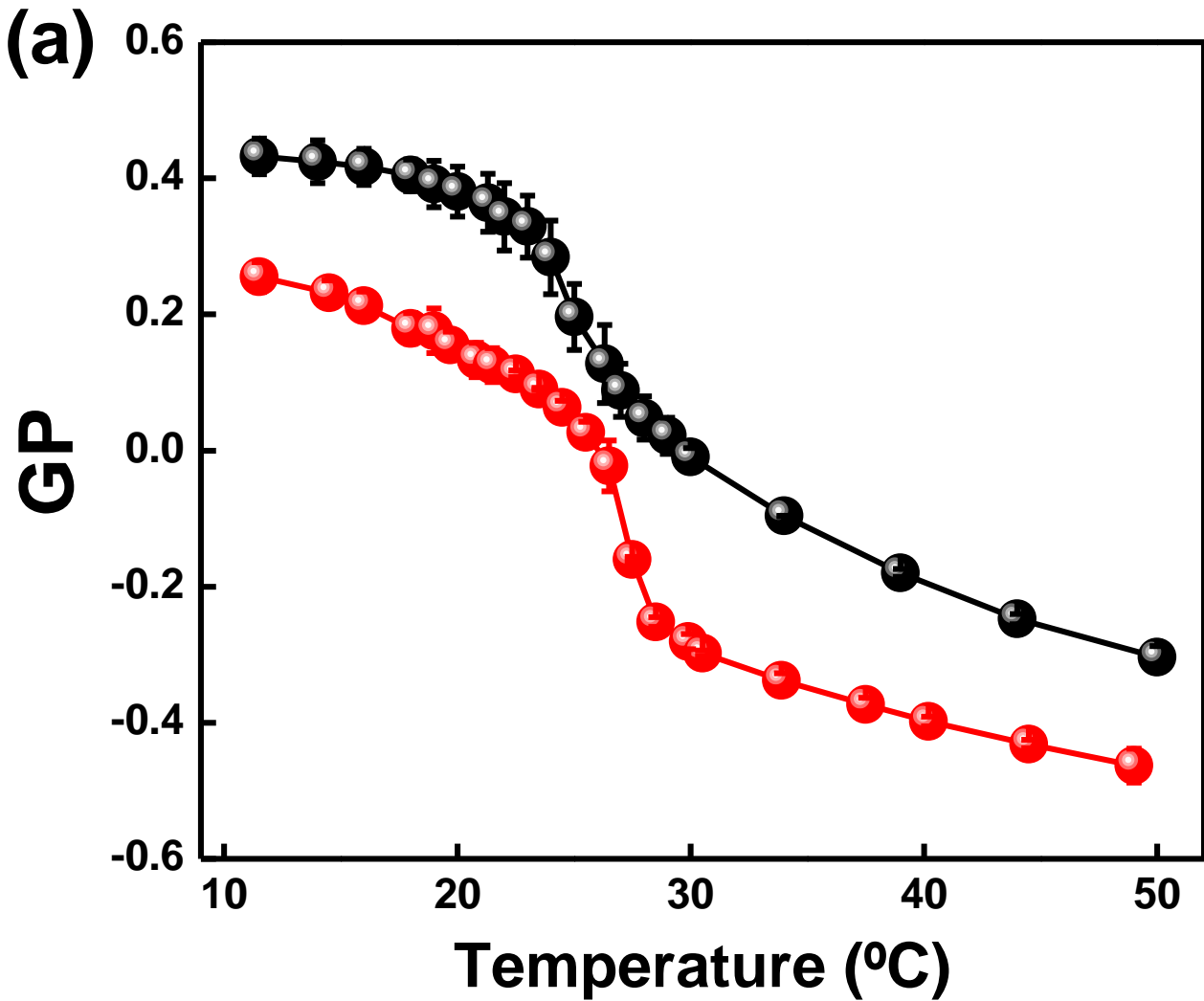
to Mesoscale Dimensions. *Langmuir* **2016**, *32* (19), 4765–4773.

(37)   Zhang, C. Note: On the Dielectric Constant of Nanoconfined Water. *J. Chem. Phys.* **2018**, *148* (15), 1–3.

(38)   Itoh, H.; Sakuma, H. Dielectric Constant of Water as a Function of Separation in a Slab Geometry: A Molecular Dynamics Study. *J. Chem. Phys.* **2015**, *142* (18), 184703.

(39)   Nagle, J. F.; Tristram-Nagle, S. Structure of Lipid Bilayers. *Biochim. Biophys. Acta - Rev. Biomembr.* **2000**, *1469* (3), 159–195.

(40)   Bagatolli, L. A. Monitoring Membrane Hydration with 2-(Dimethylamino)-6-Acylnaphtalenes Fluorescent Probes. In *Membrane Hydration*; Springer, 2015; pp 105–125.

(41)   Pérez, H. A.; Disalvo, A.; Frías, M. de los Á. Effect of Cholesterol on the Surface Polarity and Hydration of Lipid Interphases as Measured by Laurdan Fluorescence: New Insights. *Colloids Surfaces B Biointerfaces* **2019**, *178* (March), 346–351.

(42)   Leung, S. S. W.; Brewer, J.; Bagatolli, L. A.; Thewalt, J. L. Measuring Molecular Order for Lipid Membrane Phase Studies: Linear Relationship between Laurdan Generalized Polarization and Deuterium NMR Order Parameter. *Biochim. Biophys. Acta - Biomembr.* **2019**, *1861* (12), 183053.

(43)   Golfetto, O.; Hinde, E.; Gratton, E. Laurdan Fluorescence Lifetime Discriminates Cholesterol Content from Changes in Fluidity in Living Cell Membranes. *Biophys. J.* **2013**, *104* (6), 1238–1247.

(44)   Lakowicz, J. R. *Principles of Fluorescence Spectroscopy*, 3rd ed.; Springer Science+Business Media, LLC: New York, 2006.

(45)   Nickels, J. D.; Katsaras, J. Water and Lipid Bilayers. In *Subcellular Biochemistry*; 2015; Vol. 71, pp 45–67.

(46)   Parasassi, T.; Di Stefano, M.; Loiero, M.; Ravagnan, G.; Gratton, E. Influence of Cholesterol on Phospholipid Bilayers Phase Domains as Detected by Laurdan Fluorescence. *Biophys. J.* **1994**, *66* (1), 120–132.

(47)   Parasassi, T.; De Stasio, G.; Ravagnan, G.; Rusch, R. M.; Gratton, E. Quantitation of Lipid Phases in Phospholipid Vesicles by the Generalized Polarization of Laurdan Fluorescence. *Biophys. J.* **1991**, *60* (1), 179–189.

(48)   Jameson, D. M. *Introduction to Fluorescence*; CRC press, 2014.

(49)   Bacalum, M.; Zorila, B.; Radu, M. Fluorescence Spectra Decomposition by Asymmetric Functions: Laurdan Spectrum Revisited. *Anal. Biochem.* **2013**, *440* (2), 123–129.

33

(50) Bagatolli, L. A.; Parasassi, T.; Fidelio, G. D.; Gratton, E. A Model for the Interaction of 6-Lauroyl-2-(N,N-Dimethylamino)Naphthalene with Lipid Environments: Implications for Spectral Properties. *Photochem. Photobiol.* **1999**, *70* (4), 557.

(51) Wolkers, W. F.; Oldenhof, H.; Glasmacher, B. Dehydrating Phospholipid Vesicles Measured in Real-Time Using ATR Fourier Transform Infrared Spectroscopy. *Cryobiology* **2010**, *61* (1), 108–114.

(52) Rosa, A. S.; Cutro, A. C.; Frías, M. A.; Disalvo, E. A. Interaction of Phenylalanine with DPPC Model Membranes: More Than a Hydrophobic Interaction. *J. Phys. Chem. B* **2015**, *119* (52), 15844–15847.

(53) Maherani, B.; Arab-Tehrany, E.; Rogalska, E.; Korchowiec, B.; Kheirolomoom, A.; Linder, M. Vibrational, Calorimetric, and Molecular Conformational Study on Calcein Interaction with Model Lipid Membrane. *J. Nanoparticle Res.* **2013**, *15* (7), 1–17.

(54) Cseh, R.; Benz, R. Interaction of Phloretin with Lipid Monolayers: Relationship between Structural Changes and Dipole Potential Change. *Biophys. J.* **1999**, *77* (3), 1477–1488.

(55) Vollhardt, D.; Fainerman, V. B. Progress in Characterization of Langmuir Monolayers by Consideration of Compressibility. *Adv. Colloid Interface Sci.* **2006**, *127* (2), 83–97.

(56) Carrer, D. C.; Maggio, B. Phase Behavior and Molecular Interactions in Mixtures of Ceramide with Dipalmitoylphosphatidylcholine. *J. Lipid Res.* **1999**, *40* (11), 1978–1989.

(57) Cutro, A. C.; Disalvo, E. A.; Frías, M. A. Effects of Phenylalanine on the Liquid-Expanded and Liquid-Condensed States of Phosphatidylcholine Monolayers. *Lipid Insights* **2019**, *12*, 117863531882092.

(58) Clarke, R. J. Effect of Lipid Structure on the Dipole Potential of Phosphatidylcholine Bilayers. *Biochim. Biophys. Acta - Biomembr.* **1997**, *1327* (2), 269–278.

(59) Vitovič, P.; Weis, M.; Tomčík, P.; Cirák, J.; Hianik, T. Maxwell Displacement Current Allows to Study Structural Changes of Gramicidin A in Monolayers at the Air-Water Interface. *Bioelectrochemistry* **2007**, *70* (2), 469–480.

(60) Brockman, H. Dipole Potential of Lipid Membranes. *Chem. Phys. Lipids* **1994**, *73* (1–2), 57–79.

(61) Brockman, H. Lipid Monolayers: Why Use Half a Membrane to Characterize Protein-Membrane Interactions? *Curr. Opin. Struct. Biol.* **1999**, *9* (4), 438–443.
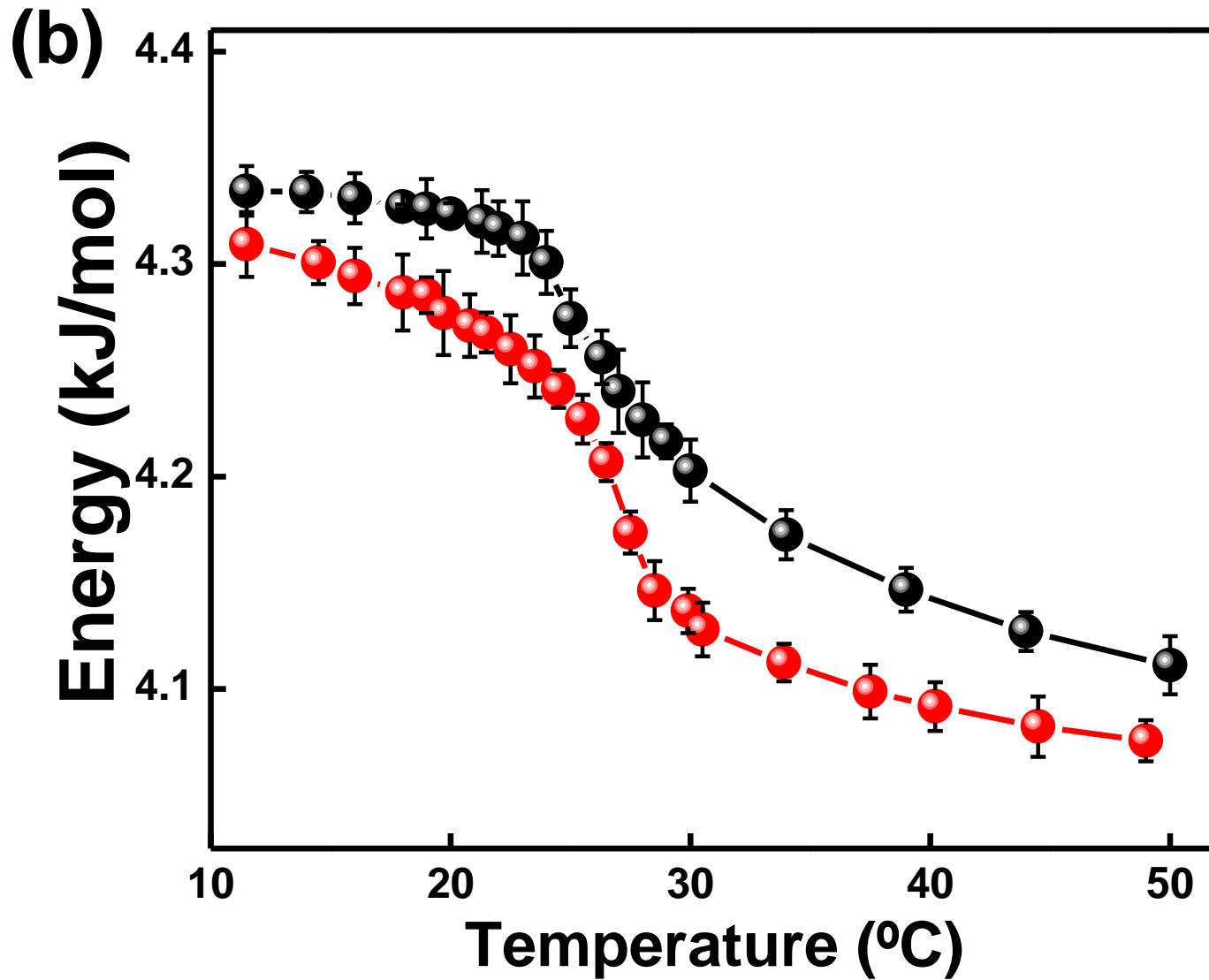
(62) Marsh, D. *Handbook of Lipid Bilayers*; CRC press, 2013.

34

(63) Blume, A. Apparent Molar Heat Capacities of Phospholipids in Aqueous Dispersion. Effects of Chain Length and Head Group Structure. *Biochemistry* **1983**, *22* (23), 5436–5442.

(64) Heerklotz, H.; Epand, R. M. The Enthalpy of Acyl Chain Packing and the Apparent Water-Accessible Apolar Surface Area of Phospholipids. *Biophys. J.* **2001**, *80* (1), 271–279.

(65) Heimburg, T. *Thermal Biophysics of Membranes*; John Wiley & Sons, 2008.

(66) Mukherjee, S.; Chattopadhyay, A. Influence of Ester and Ether Linkage in Phospholipids on the Environment and Dynamics of the Membrane Interface: A Wavelength-Selective Fluorescence Approach. *Langmuir* **2005**, *21* (1), 287–293.

(67) Ohto, T.; Backus, E. H. G.; Hsieh, C. S.; Sulpizi, M.; Bonn, M.; Nagata, Y. Lipid Carbonyl Groups Terminate the Hydrogen Bond Network of Membrane-Bound Water. *J. Phys. Chem. Lett.* **2015**, *6* (22), 4499–4503.

(68) Srivastava, A.; Malik, S.; Debnath, A. Heterogeneity in Structure and Dynamics of Water near Bilayers Using TIP3P and TIP4P/2005 Water Models. *Chem. Phys.* **2019**, *525* (March).

(69) Srivastava, A.; Karmakar, S.; Debnath, A. Quantification of Spatio-Temporal Scales of Dynamical Heterogeneity of Water near Lipid Membranes above Supercooling. *Soft Matter* **2019**, *15* (47), 9805–9815.

(70) Yu, Z. W.; Jin, J.; Cao, Y. Characterization of the Liquid-Expanded to Liquid-Condensed Phase Transition of Monolayers by Means of Compressibility. *Langmuir* **2002**, *18* (11), 4530–4531.

(71) Kučerka, N.; Tristram-Nagle, S.; Nagle, J. F. Structure of Fully Hydrated Fluid Phase Lipid Bilayers with Monounsaturated Chains. *J. Membr. Biol.* **2006**, *208* (3), 193–202.

(72) Wolfe, D. H.; Brockman, H. L. Regulation of the Surface Pressure of Lipid Monolayers and Bilayers by the Activity of Water: Derivation and Application of an Equation of State. *Proc. Natl. Acad. Sci. U. S. A.* **1988**, *85* (12), 4285–4289.

(73) Pattus, F.; Slotboom, A. J.; De Haas, G. H. Regulation of Phospholipase A2 Activity by the Lipid-Water Interface: A Monolayer Approach. *Biochemistry* **1979**, *18* (13), 2691–2697.

(74) MacDonald, R. C.; Simon, S. A. Lipid Monolayer States and Their Relationships to Bilayers. *Proc. Natl. Acad. Sci. U. S. A.* **1987**, *84* (12), 4089–4093.

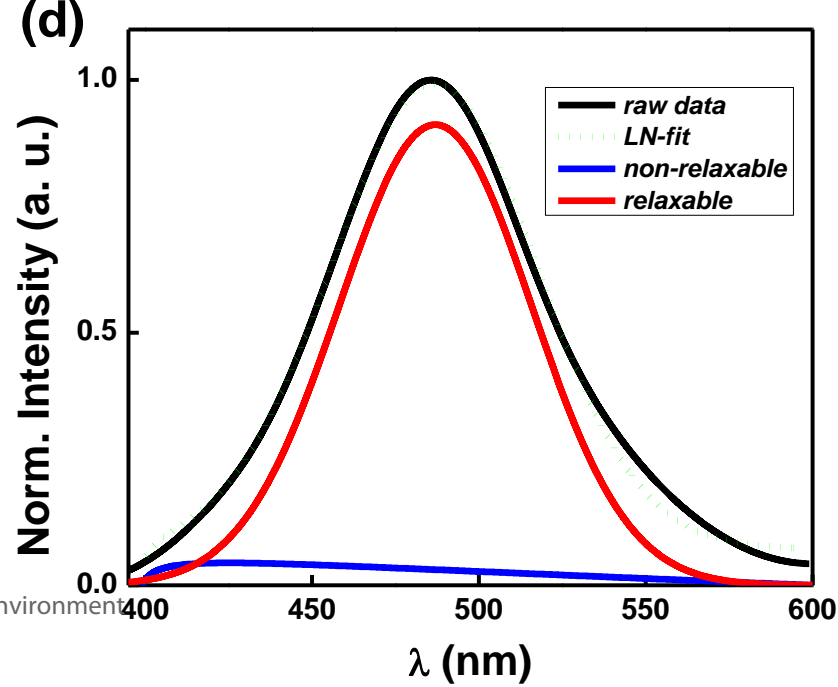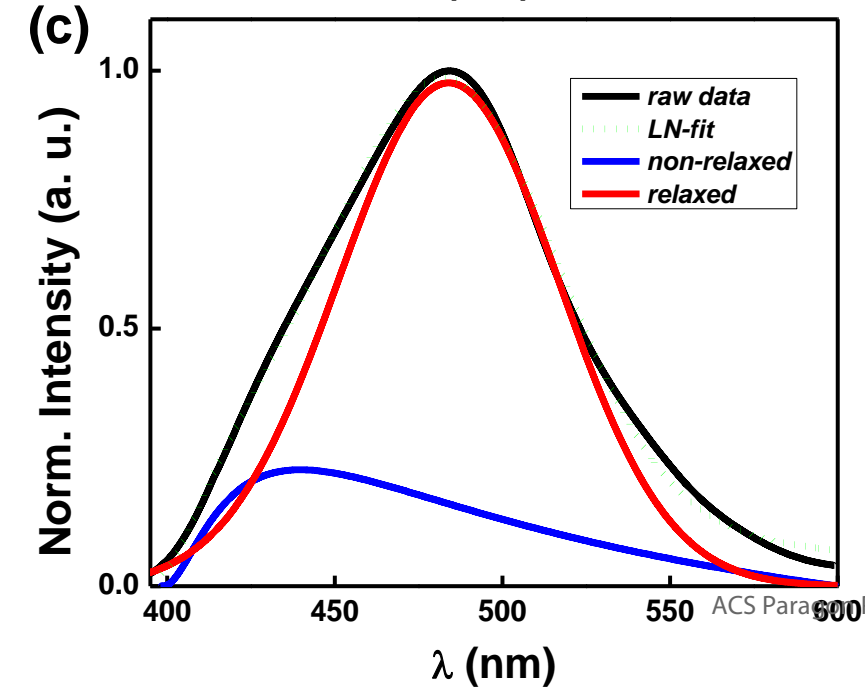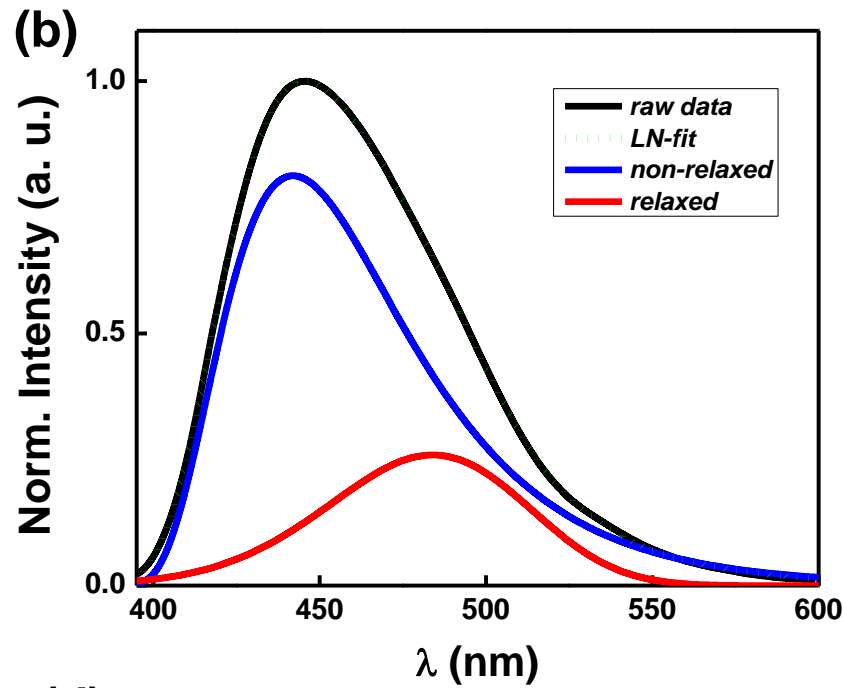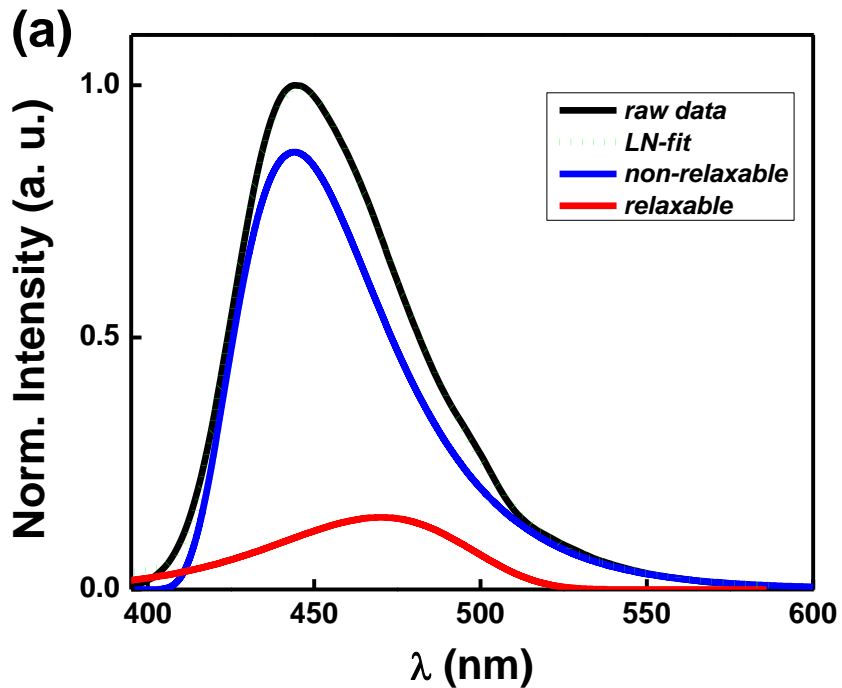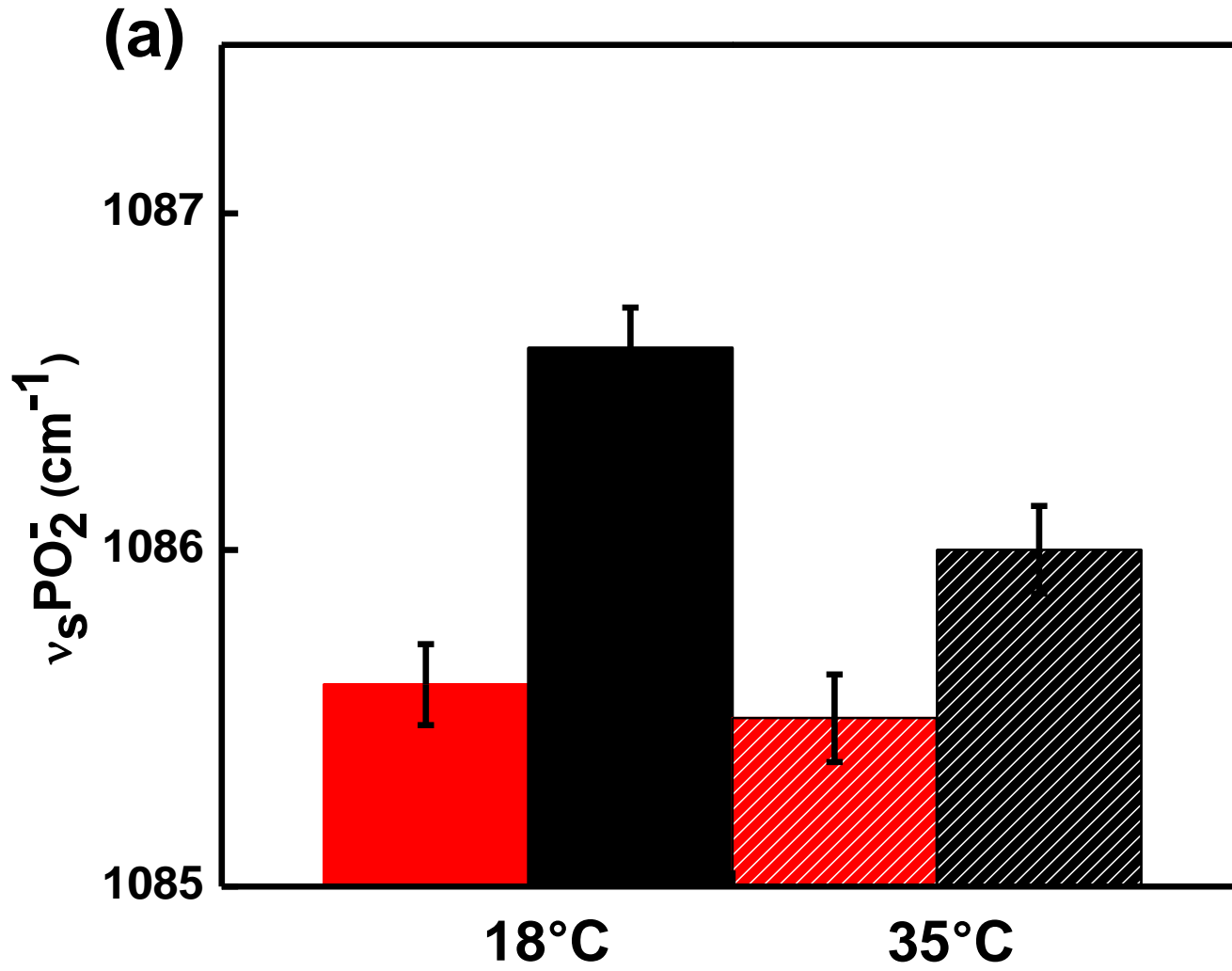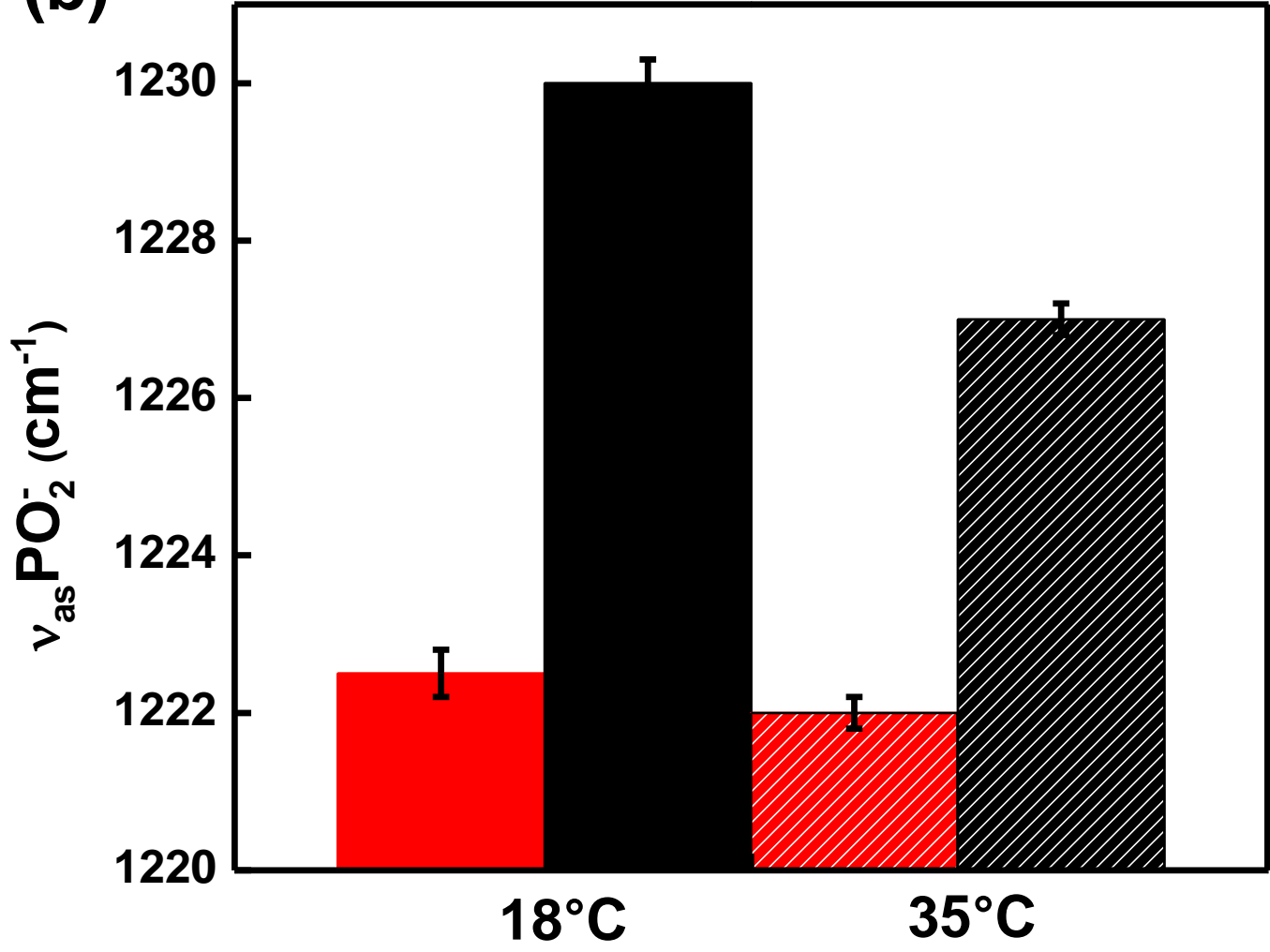**GRAPHICAL ABSTRACT**

1
2
3
4
5
6
7
8
9
10
11
12
13
14
15
16
17
18
19
20
21
22
23
24
25
26
27
28
29
30
31
32
33
34
35
36
37
38
39
40
41

(a)

1
2
3
4
5
6
7
8
9
10
11
12
13
14
15
16
17
18
19
20
21
22
23
24
25
26
27
28
29
30
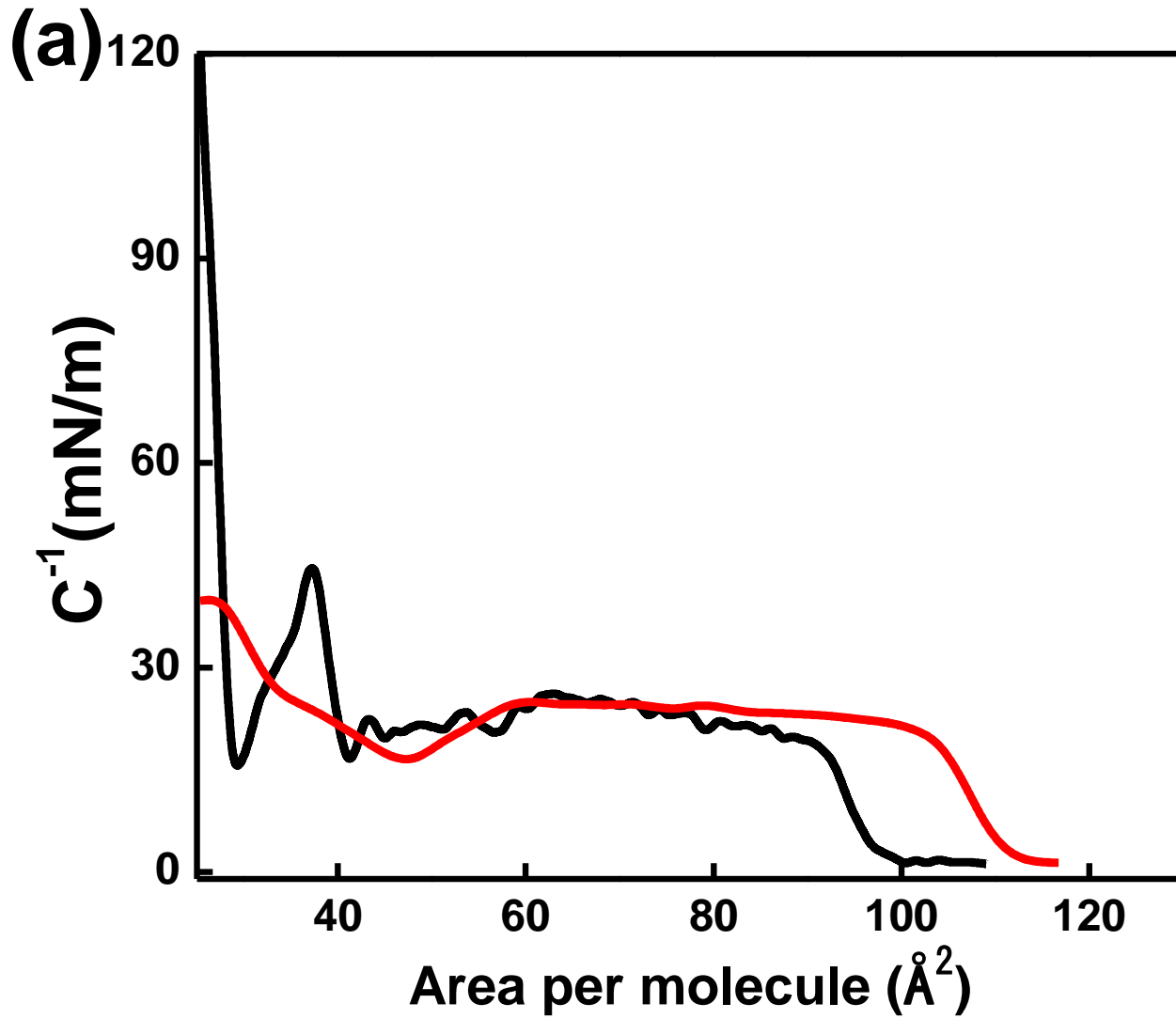31
32
33
34
35
36
37
38
39
40
41

(b)

1
2
3
4
5
6
7
8
9
10
11
12
13
14
15
16
17
18
19
20
21
22
23
24
25
26
27
28
29
30
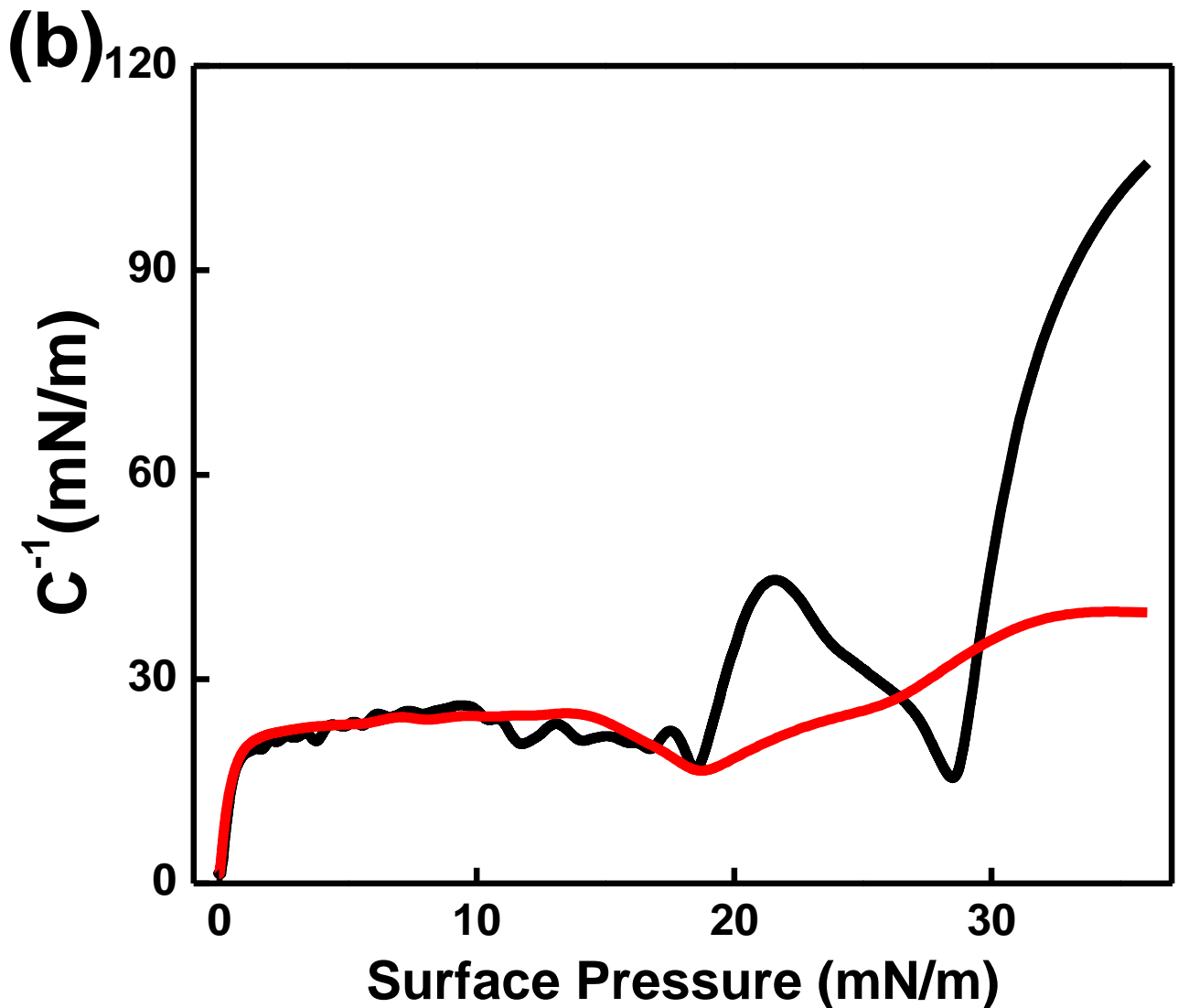31
32
33
34
35
36
37
38
39
40
41

(b)

1
2
3
4
5
6
7
8
9
10
11
12
13
14
15
16
17
18
19
20
21
22
23
24
25
26
27
28
29
30
31
32
33
34
35
36
37
38
39
40
41

(b)

1
2
3
4
5
6
7
8
9
10
11
12
13
14
15
16
17
18
19
20
21
22
23
24
25
26
27
28
29
30
31
32
33
34
35
36
37
38
39
40
41

(a)

Plot of $\nu_S PO_2^-$ (cm^{-1}) versus temperature with bars grouped at 18°C and 35°C; y-axis marked at 1085, 1086, and 1087.
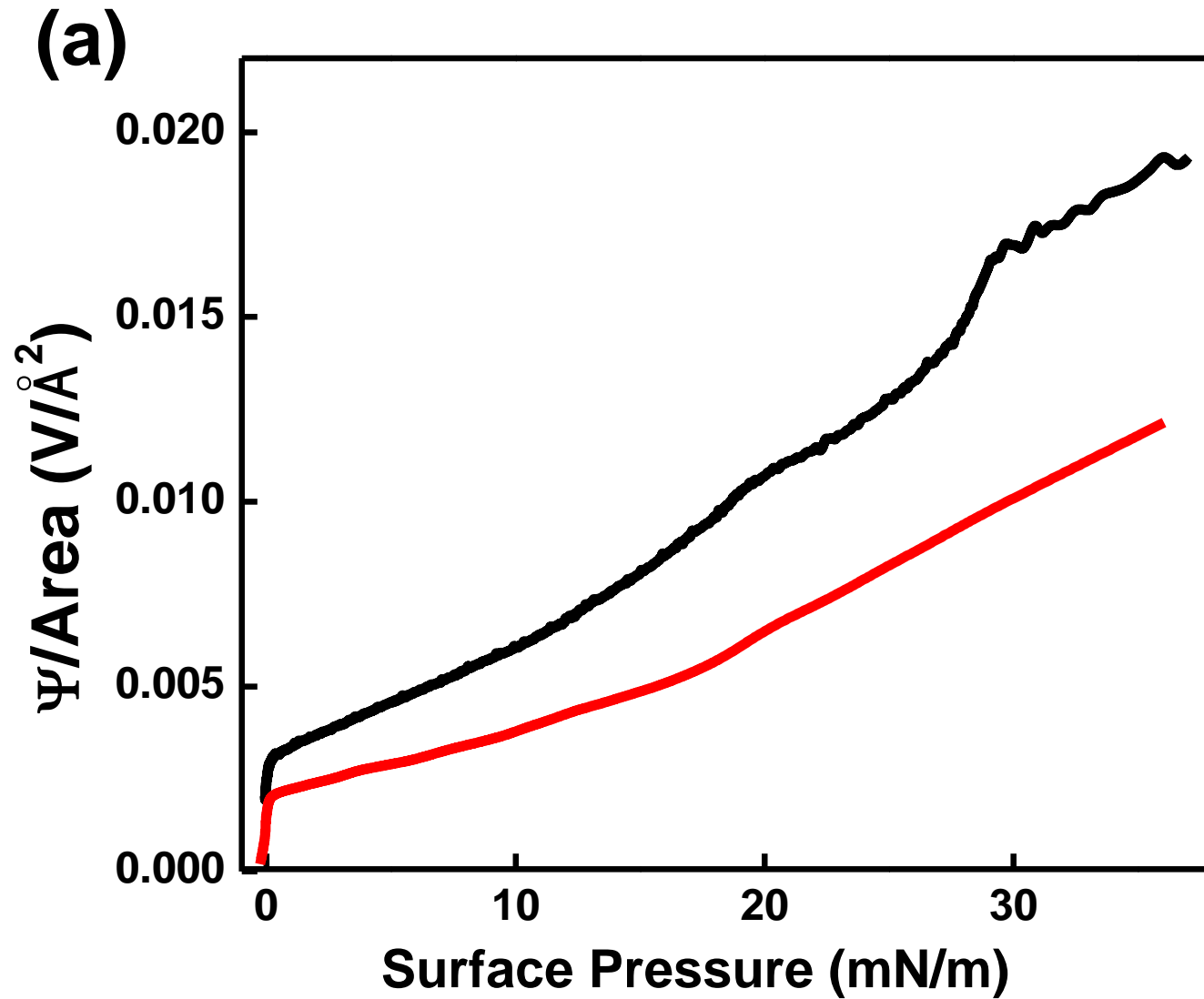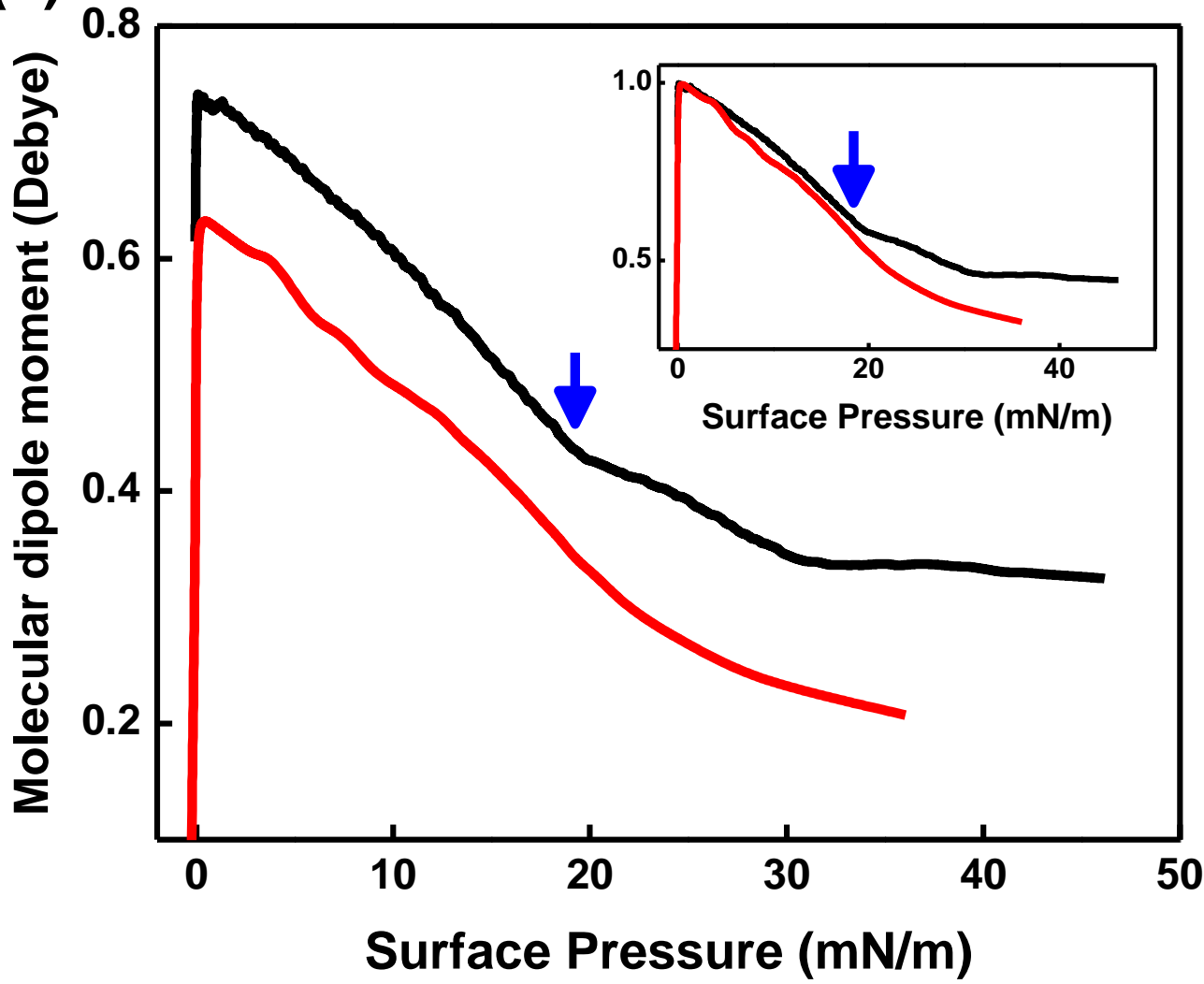
1
2
3
4
5
6
7
8
9
10
11
12
13
14
15
16
17
18
19
20
21
22
23
24
25
26
27
28
29
30
31
32
33
34
35
36
37
38
39
40
41

(b)

1
2
3
4
5
6
7
8
9
10
11
12
13
14
15
16
17
18
19
20
21
22
23
24
25
26
27
28
29
30
31
32
33
34
35
36
37
38
39
40
41

(b)

1
2
3
4
5
6
7
8
9
10
11
12
13
14
15
16
17
18
19
20
21
22
23
24
25
26
27
28
29
30
31
32
33
34
35
36
37
38
39
40
41

(a)